Localisation of equilibrative nucleoside transporter 3 (ENT3) in mouse brain

By

Lauren Emilienne Roberts

A thesis submitted to
the Faculty of Graduate Studies
in partial fulfilment of
the requirements for the degree of
Master of Science

Department of Pharmacology & Therapeutics
Faculty of Medicine
University of Manitoba
Winnipeg, Manitoba

October 2014

Abstract

Adenosine is an essential purine nucleoside of particular importance within heart and brain. The widespread and diverse actions of adenosine, driven by activation of cell surface receptors, include regulation of sleep/arousal and neuroprotective properties. The mechanisms involved in regulating adenosine concentrations remain poorly understood but are critical to signaling pathways as they determine the availability of adenosine at corresponding receptors within the extracellular space. The equilibrative nucleoside transporter (ENT) family, bi-directional, Na^+-independent nucleoside transporters, are key components in both the release and uptake of adenosine. This study has been conducted to investigate ENT3, a novel member of the ENT family. Our work has demonstrated ENT3 to be expressed throughout brain, located in cortex, cerebellum, striatum and hippocampus, at similar levels. Neurons and astrocytes, but not microglia, showed intracellular ENT3 localisation. This was confirmed by differential centrifugation, of cortex and cerebellum, which suggests ENT3 to be found within the cytoplasm.

Acknowledgments

I have been making a mental list of all the amazing people who have helped me as I worked towards completing this beast and the list has gotten rather long so before they start turning the music up and getting out the cane to yank me off the stage, I better get to it!

Dr. Fiona Parkinson is certainly top of the list; first and foremost she agreed to take me on as her student- I would not have an acknowledgements page to write if it wasn't for her! She has given up much of her time over the past two years to offer edits and suggestions to my presentations and applications, to answer my questions and to ask me many questions of her own. Her office door was always open to my random "pop-ins" and man, is she quick to reply to emails!

Wei Xiong and Dali Zhang, my fellow lab members; we may be a small group but it's a good one! Wei was such a vital key to my success here, she took me under her lab coat when I first arrived and taught me so much more than I thought I would learn. Throughout the whole process she has been a wonderful cheering section and I couldn't be luckier to have her in my corner. Dali was kind enough to perform all of my dissections, and I am truly thankful, but beyond that he was always supportive and made me feel important.

Dear KIAM. Okay, so the truth is, I didn't really want to leave Chown. I had finally learned where everything was in our lab space and had gotten comfortable! And then the news drops: we're moving. But I have to say, I was wrong. It's true, KIAM isn't perfect (not that Chown was either) but it was much more than a new lab bench. KIAM is a scientific community and it is filled with wonderful, generous people who want to help you be the best you can.

Dr. Mike Jackson (sorry, I mean Mike) and Natalie Lavine were such valuable resources for me. To properly thank Natalie would take a whole series of books (which she could add to her substantial library) but I hope she knows how much she did for me; she joined our department when I was at my lowest, with a strong love-hate relationship with science and what she later dubbed as a "black thumb" for my work, but her humor and good spirits combined with a genuine interest in my work and success (you tricky ENT3, you!) helped me pick myself up and move forward. I was always be grateful.

Dr. Tiina Kauppinen and Gary Odero, another group in KIAM that contributed to my work. Gary went far above simply donating cells, he gave up much of his own time in troubling shooting my immunostaining and offering suggestions and more than once I made him sit with me at the microscope in the dark. And, just like Natalie, Gary truly cared about my work and got genuinely excited about ENT3.

The members of Dr. Chris Andersons' lab, Dr. Jun-Feng Wangs' lab and Dr. Don Millers' lab also helped make KIAM such a great environment and hopefully the friendships I've made here will last beyond far the fourth floor.

Last, but certainly not least, my committee members, Dr. Don Miller and Dr. Barb Triggs-Raine, who was nice enough to jump on board at the end, also contributed to my success here. Dr. Miller was always a friendly face to pass in the halls, good for a quick jab with a crooked smile (yes, I need a spotlight on me at all times, thanks!) and Barb, instantly made me feel comfortable, gave up her time and offered many great suggestions and advice.

To everyone, my deepest and most sincere,

Thank you.

Dedication

"There's nothing more exciting than science. You get all the fun of sitting still, being quiet, writing down numbers, paying attention. Science has it all."

-Principal Skinner

Contents

List of Figures

List of Abbreviations

µg	micrograms
µL	microliters
ADP	adenosine diphosphate
AK	adenosine kinase
AMP	adenosine monophosphate
ATP	adenosine triphosphate
bp	base pair
BSA	bovine albumin serum
CA	cytosine β-D-arabino furanoside hydrocloride
cAMP	3', 5'-cyclic adenosine monophosphate
CD-73	ecto-5'-nucleotidase
cib	concentrative, NBMPR-insensitive, broadly selective for both purine and pyrimidine nucleosides
cif	concentrative, NBMPR-insensitive, transporter formycin B
CIP	calf intestinal alkaline phosphatase
Cit	concentrative, NBMPR-insensitive, transporter thymidine
CNS	central nervous system
CNT	concentrative nucleoside transporter
2-DG	2-deoxyglucose
ddH_2O	distilled deionized water
DMEM	Dulbecco's modified Eagle medium

DMSO	dimethyl sulphoxide hybrid-max
cDNA	complimentary deoxyribonucleic acid
DNA	deoxyribonucleic acid
dNTP	deoxynucleotide triphosphates
DPR	dipyridamole
DTT	dithiothreitol
E. coli	*Escherichia coli*
EDTA	ethylene diamine tetra-acetic acid
EGTA	ethylene glycol tetra-acetic acid
ei	equilibrative nucleoside transporter insensitive to NBT1 inhibition
ENT	equilibrative nucleoside transporter
EPSC	excitatory postsynaptic current
es	equilibrative nucleoside transporter sensitive to NBT1 inhibition
FBS	fetal bovine serum
FITC	fluorescein isothiocyanate
G_i/G_o	inhibitory G proteins
G_s	stimulatory G protein
GABA	gamma-aminobutyric acid
GAPDH	glyceraldehyde 3-phosphate dehydrogenase
GDP	guanosine-5'-diphosphate
GFAP	glial fibrillary acidic protein
GPCR	G-protein coupled receptor
GTP	guanosine-5'-triphosphate

HBSS	Hanks balance salt solution
HEPES	4-2-hydroxyethyl-1-piperazineethanesulfonic acid
HEK293T	human embryonic kidney 283, expressing SV40 large T antigen
hENT	human equilibrative nucleoside transpoter
HX	hypoxanthine
ICC	immunocytochemistry
IgG	immunoglobulin G
INO	inosine
IRES	internal ribosome entry site
LB	Luria-Bertani
Kb	kilo base pairs
kDa	kilodaltons
MEM	minimum essential media
mENT	mouse equilibrative nucleoside transporter
MICB	Manitoba Institute of Cell Biology
mL	milliliters
mM	millimolar
mins	minutes
mRNA	messenger ribonucleic acid
MW	molecular weight
NAD	nucleoside analog drug
NBMPR	S-(4-nitrobenzyl)-6-thioinosine
NeuN	neuronal nuclei

ng	nanograms
NP-40	Non-idet 40 buffer
NT	nucleoside transporter
PCR	polymerase chain reaction
PBS	phosphate buffered saline
PHID	pigmentary hypertrichosis and insulin-dependent diabetes mellitus
PMAT	plasma membrane monoamine transporter
PMSF	phenylmethylsulfonyl fluoride
Puro	puromycin
PVDF membrane	polyvinylidene fluoride membrane
RE	restriction enzyme
rpm	revolutions per minute
RT	room temperature
Rt	reverse transcription
Rt-PCR	reverse transcription polymerase chain reaction
RNA	ribonucleic acid
sec	seconds
SDS	sodium dodecyl sulfate
SDS-PAGE	sodium dodecyl sulfate polyacrylamide gel electrophoresis
SNP	single-nucleotide polymorphism
SOC medium	super optimal broth with catabolic repression
TBS	Tris-buffered saline
TBS-T	Tris-buffered saline with tween

Tween-20	polyoxyethylene-sorbitan monolaurate
UV	ultraviolet
V	volts
WT	wild type
Xa	xanthine

Chapter 1

Introduction

1.1 Adenosine and the CNS

Purines are essential constituents of all living cells and important molecules not only involved in purinergic signaling pathways but are essential components to cellular function (Haystead, 2006). Also referred to as the purinome, purinergic signaling involves purine nucleotides and nucleosides, corresponding receptors, enzymes, channels and transporters that all work cooperatively to modulate cellular function, homeostasis and responses (Volonte and D'Ambrosi, 2009). One such purine nucleoside is adenosine; found throughout the body, along with its corresponding receptors, adenosine is of particular importance in the heart and brain (Burnstock, 1972; Drury and Szent-Gyorgyi, 1929).

Over the years studies have demonstrated the direct involvement of adenosine in vital CNS processes (Phillis and Wu, 1981) including, but not limited to, modulating cellular metabolism, anticonvulsant actions (Dunwiddie, 1999), regulation of sleep and arousal (Huston et al., 1996; Landolt, 2008) and regulation of pain signal transmission (DeLander

and Hopkins, 1986; Post, 1984). All physiological actions of adenosine rely on the activation of specific adenosine receptors (Sebastiao and Ribeiro, 2000). Classified as P1 purinergic receptors, four distinct adenosine receptors have been identified to date; A_1, A_{2A}, A_{2B} and A_3, all of which are seven-transmembrane domain G-protein coupled receptors (GPCR) (Fredholm et al., 2001; Lefkowitz, 2004). Adenosine, binding to the extracellular site of the adenosine receptor, activates the guanine nucleotide exchange factor of the associated G-protein resulting in the release of a GDP molecule and the binding of a GTP molecule to the G_α subunit. The presence of a GTP molecule induces a conformational change in the G_α subunit, which then dissociates from the $G_{\beta\gamma}$ subunits and activates further downstream pathways.

Although each adenosine receptor shares a common structure, their downstream effects within the cell can be very different and are determined, in part, by the type of associated G-proteins. The two main effects of adenosine signaling can be classified as inhibitory and excitatory (Correia-de-Sa et al., 1996; Cunha et al., 1994). A_1 and A_3 receptors, considered to primarily induce inhibitory actions (Brand et al., 2001), are predominantly linked to $G_{i/o}$ proteins which act by inhibiting adenylyl cyclase thereby decreasing cAMP concentration. In contrast, A_{2A} and A_{2B} receptors, largely considered excitatory, are associated primarily to G_s proteins, which activate adenylyl cyclase resulting in increased concentration of cAMP. Although both are involved in excitatory signaling, A_{2A} and A_{2B} receptors differ in that A_{2A} is found primarily expressed in the CNS and A_{2B} within the PNS (Svenningsson et al., 1999). The presence of multiple distinct adenosine receptors, linked to both stimulatory and inhibitory signaling pathways, is a good indicator as to adenosines' enormous signaling potential.

One of the most compelling signaling properties of adenosine within the CNS, in terms of its therapeutic potential, is its neuroprotective actions (Cunha, 2005). It has been many years since it was first demonstrated that extracellular adenosine concentrations rise drastically in unfavorable and stressful conditions such as during hypoxia (deprivation of oxygen) and ischemia (deprivation of oxygen and glucose) (Safran et al., 2001). Observations of increased extracellular adenosine, and resulting neuromodulatory effect in neighbouring cells, in such conditions have led to the use of the term 'retaliatory metabolite' when describing adenosine (Newby, 1984).

1.2 Regulation of Adenosine Concentration

For many years, adenosine was thought to only be released by cells under pathological conditions. As science and laboratory techniques have advanced, continued and in-depth studies have demonstrated clearly that adenosine is released as a result of normal physiological activity as well as during pathophysiological states. Although understanding of the signaling pathways and receptors of adenosine have been well documented, the mechanisms involved in regulating extracellular adenosine concentration remain poorly understood. As each signaling cascade is initiated by adenosine binding to the extracellular binding site of corresponding receptors and ends by clearing adenosine from the extracellular matrix, the importance of regulating extracellular adenosine concentrations should not be underestimated. The difficulty in studying these mechanisms is due primarily to the num-

ber of intersecting pathways of adenosine formation and release; altering activity, expression or localisation of one component results in compensatory responses in another making it difficult to assess individual roles of enzymes and transporters.

Below offers the most current descriptions of known mechanisms by which adenosine is produced and extracellular concentrations are regulated within cells; they have been classified as intracellular pathways and extracellular pathways.

1.2.1 Intracellular Pathways

There exist a number of nucleotides, found within the intracellular space, that are adenosine precursor molecules and as such, they can be metabolized to form adenosine. It was previously believed that direct adenosine release was only as a result of pathophysiological conditions but more recent studies have demonstrated adenosine to be released in physiological conditions. The direct release of adenosine is dependent on the intracellular production pathways and therefore, the factors and conditions that influence intracellular adenosine concentration are of great importance to understanding adenosine signaling (Brundege and Dunwiddie, 1998).

There are currently two general mechanisms of direct adenosine release; intracellularly formed adenosine can accumulate and be released via facilitated nucleoside transporters (NTs) expressed at the cell membrane that transport adenosine in a concentration gradient dependent manner or alternatively, evidence is accumulating demonstrating direct adenosine release via exocytosis in a variety of brain structures.

The production of intracellular adenosine is due in part to the activity level of the cell through the simple consideration that an increase in activity would result in an increased

consumption of ATP resulting in the formation of adenosine via intracellular enzymatic activity. As adenosine is unable to cross cell membranes nucleoside transporters facilitate the direct release of adenosine as intracellular concentrations increase. Two families of nucleoside transporters have been identified to date, the concentrative nucleoside transporter family (CNT) and the equilibrative nucleoside transporter family (ENT). Although both CNTs and ENTs are considered important components in nucleoside salvage pathways, the ENT family plays critical roles in physiological processes within brain by modulating extracellular adenosine concentrations (Baldwin et al., 1999). Due to the neuromodulatory effects of adenosine, the link between neural activity and the production of intracellular adenosine for release into the extracellular space, holds great interest.

Although defined simply as a chemical signal that is released into the synaptic cleft which separates two neurons, any substance that is classified as a neurotransmitter must fulfil the following three criteria; the substance must be found within the presynaptic neuron (presence), the release of the substance must be Ca^{+2}-dependent and directly linked to presynaptic depolarization (the release) and finally, the postsynaptic cell must be found to express the receptors corresponding to the substance (postsynaptic effects). Currently adenosine is not considered a true neurotransmitter as previous studies were not able to demonstrate adenosine release from presynaptic neurons was the result of depolarization, although more recent evidence opposes this classification (Corti et al., 2013; Song et al., 2014; Wall and Dale, 2013).

In a number of studies, adenosine has now been demonstrated to be released directly through exocytosis. Electrical stimulation of cerebellar slices and area CA1 of hippocampal slices showed adenosine release to be both sensitive to Ca^{+2} and action potential dependent

using tetrodotoxin, a neurotoxin that inhibits action potential (Wall and Dale, 2007, 2013). A study at the calyx of Held within the brainstem demonstrated adenosine release to be independent of ectonucleotidases, which when inhibited did not have an effect on measured excitatory postsynaptic currents (EPSC) (Wong et al., 2006).

In addition, preferences as to the primary mechanism of adenosine release have been found to differ between cell types. For example, it has been previously demonstrated that astrocytes express much higher levels of adenosine kinase (AK) as compared to neurons (Gouder et al., 2004). This is of importance as AK is responsible for the phosphorylation of intracellular adenosine to form AMP whereby AK activity maintains very low intracellular concentrations of adenosine. Due to high AK expression, direct adenosine release by astrocytes has not been found to be an important source of extracellular adenosine. In contrast, intracellular adenosine levels within neurons can increase due to high metabolic demand and low AK expression whereby adenosine is released by ENT isoforms, directing adenosine efflux following the concentration gradient (Brundege and Dunwiddie, 1998).

Studies of tissues have also shown that multiple intersecting pathways can be involved in adenosine regulation and preference can vary in different tissues throughout the brain. For example, two separate studies were performed on cerebellar slices and hippocampal slices and although both were found to release adenosine by exocytosis, further studies were performed to determine the role of ENTs in adenosine release; inhibiting cerebellar slices with ENT1 and ENT2 inhibitors had no effect on adenosine release indicating a distinct mechanism of release (Wall et al., 2007) whereas blocking ENT1 and 2 in hippocampal slices significantly reduced the amount of adenosine release, indicating ENTs are involved in adenosine release from hippocampal cells (Wall and Dale, 2013).

Although this is just one example in which distinct mechanisms of adenosine regulation can be present simultaneously, it is certainly not the only case and as such studies on adenosine release remain unresolved. It is clear that tissue, cell type and stimulus are all factors that influence adenosine release (Latini and Pedata, 2001). NTs have garnered much attention over the years. Although expression studies of NTs show widespread distribution throughout the CNS, a direct link between NT isoforms and adenosine signaling has yet to be identified. Currently, NTs are considered primarily responsible for adenosine reuptake rather than a mechanism of adenosine release albeit NTs are still important components in adenosine signaling (Stone et al., 2007). There are two known NT families, classified as CNT and ENT, which will be further examined as they differ by their localisation, abundance and substrate specificity. Consequently, the impact of each NT isoform on adenosine signaling is determined by such properties.

1.2.2 Extracellular Pathways

Adenosine can also be released indirectly through the metabolism of released ATP or ADP by enzymes found within the extracellular space. Classified as ectoenzymes, a number of extracellular enzymes have been found to be expressed within the CNS; nucleoside triphosphate diphosphohydrolases (NTPDases), ectonucleotide pyrophosphatase/phosphodiesterases and ecto-5'-nucleotidase, which together contribute to the formation of adenosine, through sequential hydrolysis (Langer et al., 2008; Zimmermann, 1996). Jointly these enzymes act to control and regulate the availability of adenosine at the corresponding receptors and contribute to the salvage and recycling processes as the final metabolites can then be transported back into the cell by specific transporters (Langer et al., 2008). Not

surprisingly, the hydrolysis pathways in the catabolism of extracellular nucleotides is complex as the multiple enzyme families have different functional and molecular properties and expression profiles.

Even though the presence of ectoenzymes, responsible for the degradation of ATP, within the CNS has been previously demonstrated, this does not directly indicate that the formation of adenosine from released ATP is a critical route of adenosine production in physiological signaling pathways (Lovatt et al., 2012). Studies have been conducted in hopes of separating NT activity from ectoenzymatic activity to identify the predominant source of adenosine, be it the direct release or through enzymatic action, but this has proven difficult for a number of reasons. For example, amounts of ATP released into the extracellular space are small and extremely difficult, if not impossible, to detect with current techniques (Frenguelli et al., 2007).

Although ATP is a known neurotransmitter, initiating a cellular response at distinct receptors, it has also been considered an important source of extracellular adenosine although this may not be accurate in all cell type. A recent study has demonstrated that ATP is not a true source of extracellular adenosine in neurons, under physiological conditions, as released ATP is not degraded to produce adenosine in high enough concentrations to induce a receptor mediated response (Lovatt et al., 2012). It is suggested that previous studies had inundated the extracellular space with exogenous ATP which would saturate the normal adenosine uptake and clearance mechanisms resulting in activation of signaling pathways that are not normally active (Lovatt et al., 2012). This group has used multiple alternative approaches to further explore the source of adenosine in synaptic depression,

and consistently, in numerous situations showed that degradation of ATP in the extracellular space was not responsible for adenosine receptor activation and that neurons release adenosine directly through ENT isoforms (Lovatt et al., 2012).

1.3 Nucleoside Transporters

Any signaling pathway can be broken down simply into three distinct parts; signal initiation where by the ligand is formed or released to the site of its receptors, activation of the corresponding receptor resulting in transmission of a signal within the target cell and termination of signal at which point the ligand is metabolized or removed from the receptor which returns to an inactive state. With ample research over the last eighty years, adenosine signaling within the CNS has been well characterized in terms of receptors involved and their effects following activation by adenosine. In contrast, the mechanisms involved in releasing and removing extracellular adenosine in signaling pathways are far less known. Although attempts have been made to investigate these processes, studies are difficult to conduct for a variety of reasons. The mechanisms involved are complex, involving numerous enzymes, substrates and transporters and the mechanisms of release seem to be stimulus, cell- and tissue-type dependent. Furthermore, as multiple intersecting pathways have been identified, attempts to study one specific method often results in compensatory responses from another release method, making it extremely difficult to assess the activity of a particular mechanism. As laboratory techniques and tools improve studies will become more specific and sensitive enabling more precise studies.

One known mechanism of regulating extracellular adenosine concentrations is via the action of NTs, as mentioned previously. All nucleosides, composed of a nitrogenous base attached to a five-carbon sugar, are hydrophilic compounds and as a result they are unable to cross plasma membranes without an appropriate transporter protein. There are two known, evolutionarily unrelated, families of NTs; CNTs and ENTs which are encoded by the SLC28 gene family and the SLC29 gene family, respectively, and which differ by their mechanism of substrate translocation. The ENT and CNT families are evolutionarily ancient and no sequence or structural similarities exist between these two families. Both NT subtypes are widely expressed and in many instances, a single cell has been found to co-express multiple ENT and CNT isoforms. It is interesting to note that in comparison of either hENTs and hCNTs to other known transporter proteins, both NT subtypes are subjected to very infrequent genetic variations (Osato et al., 2003; Young et al., 2013).

Currently, the principal physiological role of all NTs is thought to be in nucleoside salvage pathways. Although the majority of cells are capable of de novo synthesis to form nucleosides as required by the cell, recycling nucleosides by salvage pathways using NTs requires far less energy and therefore recycling processes are favored by cells. In contrast, some cells do not express the necessary enzymes required for de novo synthesis and as such they are completely reliant on salvage pathways as their source of nucleosides, the vital building blocks of numerous cellular components and critical signaling molecules in many cellular processes. The CNS is known to have limited capacity for de novo biosynthesis of purines and pyrimidines and consequently NTs are especially important to maintain proper cell function within the brain (Griffith and Jarvis, 1996).

More recently, the role of certain NT subtypes in processes other than nucleoside salvaging has become important, in particular the contribution of NTs in signaling pathways. Studies of the mechanisms of regulating signaling have shown, if nothing else, that they are complex and involve numerous components and intersecting pathways which work together to maintain strict control of nucleoside signaling molecules, such as adenosine. Understanding the localisation, abundance, specificity and activity of each NT subtype will help determine their specific contributions to signaling pathways, with an emphasis on the impact of such properties to adenosine signaling within brain.

1.3.1 Concentrative Nucleoside Transporter (CNT) Family

Encoded by the SLC28 gene family, there are currently three known members of the CNT family identified as CNT1-3. CNT isoforms have been found to be expressed in eukaroytes and eubacteria but not in plants. The CNT family shares certain common characteristics; first of all, CNTs are Na^+-dependent transporters, which means that the accepted permeants are transported in a unidirectional manner, coupled to the sodium concentration gradient. Although substrate specificity of each CNT isoform will vary, all nucleoside permeants will be transported into the cell, together with sodium, as extracellular sodium concentrations are higher than intracellular concentrations. Secondly, topology has been proposed based on comparisons to known proteins with similar amino acid sequences and is suggested to be conserved between the three isoforms to contain 13 transmembrane domains, an extracellular C terminus and a cytoplasmic N terminus (Kong et al., 2004). Current consensus suggests CNTs to be primarily involved in nucleoside salvage pathways and are

highly expressed in a tissue-specific fashion, primarily rapidly growing cells, such as cancer cells, suggesting an important role in contributing to and maintaining nucleoside pools for various processes of cell growth, such as DNA replication (Gray et al., 2004; Valdes et al., 2002).

Further studies of CNTs have found little evidence of their involvement in adenosine signaling within brain. Although adenosine is a known substrate of CNT isoforms, in particular CNT2, their physiological function may be quite different to that of the ENT family. CNT2 expression and activity has been demonstrated within the blood brain barrier (BBB) and is considered the principle mechanism of BBB adenosine transport, enabling the Na^+-dependent influx of adenosine to brain (Li et al., 2001). Due to the rapid inactivation of blood-borne adenosine by circulating enzymes, no signaling effects are observed as a result of CNT2 activity at the BBB (Li et al., 2001). Regional differences in distribution and expression profile of NTs are a good indication of their physiological functions. Comparisons of CNT and ENT distributions show ENT isoforms to be much more broadly distributed within brain suggesting ENTs to be essential in regulating various signaling cascades and physiological responses and CNTs to play a functionally distinct role (Lu et al., 2004).

1.3.2 Equilibrative Nucleoside Transporter (ENT) Family

The SLC29 gene family, an evolutionarily old family, is found to be expressed only within eukaroytes, encoding the ENT family of transporters comprised of 4 known isoforms identified as ENT1-4. In contrast to the previously mentioned CNT family, ENT isoforms are widely expressed, bi-directional, Na^+-independent transporters although more recent studies suggest newly identified ENT isoforms may be proton gradient-driven transporters. All

four members of the ENT family have been found within brain; as ENT3 and 4 have been far less studied, their functional and tissue distribution profile is less well-known. The crystallographic structure of the ENT family has yet to be determined however comparisons of the amino acid sequence with other known proteins predicts a topology of 11 transmembrane domains with an extracellular C terminus and a cytoplasmic N terminus (Sundaram et al., 2001).

ENTs are thought to be involved in nucleoside salvage pathways and have important therapeutic implications in the transport of nucleoside and nucleobase analogs that are currently used as anticancer and antiviral agents. Although the substrate specificity of each ENT isoform is slightly different, they have each been shown to transport adenosine in some capacity. In part due to the bidirectional, facilitated transport properties of the ENT family, they are considered key components in adenosine signaling pathways. Unlike the CNT family, ENT isoforms do not require energy but instead transport their permeants based solely on their individual concentration gradient across the cell membranes whereby permeants are moved from the side of higher concentration to lower. As such ENTs participate in both the influx and efflux of nucleosides and depending on their abundance and localisation, are directly linked to adenosine signaling. The role of each ENT isoform in adenosine signaling should be assessed individually.

As ENT1 and 2 were the first ENT isoforms to be identified, the majority of studies have focused on them. ENT1 and 2 have been best characterized in part due to their localisation on the plasma membrane and the identification of vital biological tools that enable specific studies. Discovered within the past 15 years, once the human genome project was completed, ENT3 and 4 remain poorly understood. In comparison to ENT1 and 2, they are

harder to study; there are no known inhibitors to enable studies of their functional roles and there is a lack of commercial antibodies with evidence of target specificity. Additionally, according to some reports (Baldwin et al., 2005; Barnes et al., 2006; Govindarajan et al., 2009; Hsu et al., 2012), they are thought to be intracellular transporters and as such determining both their function and substrate specificity is difficult.

To further understand adenosine signaling, attention has turned to investigating the mechanisms involved in regulating extracellular adenosine concentrations and the impact on signaling cascades.

1.3.2.1. ENT1

hENT1 (SLC29A1), the first member of the ENT family to be identified, is composed of 456 amino acid residues. Initial studies identified a nucleoside transporter that was potently inhibited by nitrobenzylthioinosine (NBMPR) (Crawford et al., 1998). Distribution studies of human brain determined hENT1 to be most highly expressed in cerebral cortex, followed by temporal and occipital brain regions with lowest expression in hippocampus, medulla, pons and cerebellum (Jennings et al., 2001). Although ENT1 is considered to be primarily expressed on the plasma membrane, ENT1 has also been found intracellularly localised on nuclear membranes, endoplasmic reticulum and mitochondrial membranes (Lai et al., 2004; Mani et al., 1998).

Due to the availability of pharmacological and molecular tools, ENT1 remains the best characterized member of the ENT family and is considered the primary cellular mechanism responsible for nucleoside uptake both in terms of physiological processes and therapeutic

agents. Ubiquitously expressed, hENT1 is permeable to a wide range of purine and pyrimidine nucleosides while direct studies of transport kinetics have measured a K_m value for adenosine of 0.05mM (Ward et al., 2000). Studies to assess the role of hENT1 in adenosine signaling in brain have been attempted through co-localisation studies with A_1 receptors. A similar distribution pattern was revealed, suggesting hENT1 is directly involved in regulating the neuromodulatory actions of adenosine linked to A_1 receptor activity (Jennings et al., 2001).

1.3.2.2. ENT2

The second member of the ENT family to be identified, hENT2 (SLC29A2), a 456-residue protein, was discovered based on the insensitivity of hENT2 to inhibition by NBMPR (Crawford et al., 1998). Initial studies identified two similar transporters that were differentiated by their sensitivity to NBMPR; at this time the transporters were classified as "*es*" for equilibrative sensitive and "*ei*" for equilibrative insensitive (Crawford et al., 1998). It was not until after sequencing that these transporters were discovered to be coded by the *SLC29* gene family and were renamed ENT1 and ENT2 respectively. Despite differences in NBMPR sensitivity, hENT1 and hENT2 share many common properties; both are predominately expressed at the cell surface, have similar substrate selectivity and similar tissue distribution profile, although skeletal muscle has been shown to have the highest level of hENT2 expression (Crawford et al., 1998; Jennings et al., 2001). Distribution studies of hENT2 within brain have determined cerebellum and brainstem to express the highest lev-

els of hENT2 followed by the medulla and thalamus and finally cerebral cortex, hippocampus and basal ganglia were found to have the lowest levels of expression (Jennings et al., 2001).

The overlap in both substrate specificity and expression profiles have made studies separating the functional role of hENT1 and 2 difficult. In comparison to hENT1, hENT2 is classified as a low affinity nucleoside transporter as kinetic studies have determined hENT2 to have generally lower affinities for endogenous nucleosides than hENT1. An exception is inosine, for which hENT2 has a 4-fold higher affinity (Ward et al., 2000). This functional difference could be one possible explanation for why these two closely related isoforms are often found to be co-expressed in many cell types. It also suggests an important role of hENT2 in the uptake of adenosine metabolites in muscle cells in energy depleting conditions (Ward et al., 2000). Similarly to hENT1, co-localisation studies were performed comparing the expression profiles of hENT2 to A_1 receptors within brain to assess the role of hENT2 in adenosine signaling; results from this study did not show a correlation in expression profiles between hENT2 and A_1 receptor (Jennings et al., 2001).

1.3.2.3. ENT3

Also known as SLC29A3, hENT3 was first identified by BLAST algorithm GenBank sequence databank search in 2001, after completion of the human genome project (Hyde et al., 2001). Classified as the third member of the ENT family based on sequence homology and composed of 475 amino acid residues, hENT3 differs from the previously characterized ENT members by three unique properties. First of all, initial studies of the hENT3 amino acid sequence revealed a 51-residue, N-terminal hydrophilic region that is not found

within the amino acid sequence of other ENT isoforms (Hyde et al., 2001). Secondly, although the precise localisation of ENT3 has not yet been conclusively confirmed, current studies suggest it to be an intracellular transporter (Baldwin et al., 2005; Govindarajan et al., 2009; Hsu et al., 2012). Lastly, although all members of the ENT family are Na^+-independent transporters, recent findings suggest ENT3 transport activity to have a strong pH dependence (Baldwin et al., 2005).

Tissue distribution studies of hENT3, based on RNA expression, have indicated a widespread distribution pattern with highest expression in placenta, uterus, ovary, spleen, lymph node and bone marrow, and lowest expression in both the brain and heart (Baldwin et al., 2005). Preliminary studies of subcellular distribution of ENT3 suggests localisation to be cell-type dependent, observed expression patterns include cell surface, cytoplasmic distribution and seemingly vesicular staining (Govindarajan et al., 2009). The N-terminal region of ENT3 contains motifs similar to that of known endosomal/lysosomal targeting motifs (Bonifacino and Traub, 2003). Site specific mutations within the N-terminal region were performed to assess the importance of this unique region in cellular trafficking processes; such mutations resulted in the abnormal expression of hENT3 at cell surface. Based on such experiments the N-terminal region is considered critical in proper trafficking of hENT3 (Baldwin et al., 2005).

Due in part to the lack of molecular and pharmacological tools, such as antibodies and inhibitors, studies of ENT3 are rare. Furthermore, as initial studies of hENT3 have demonstrated it to be predominantly an intracellular transporter, found on the mitochondrial, lysosomal and endosomal membranes, ENT3 was not previously thought to significantly contribute to signaling pathways as opposed to ENT1 and 2, which have been found to be

predominantly expressed on the cell surface. In addition, the pH dependent transport by ENT3 is thought to reflect the intracellular localisation, for example within lysosomes that have a low pH, in salvage pathways rather than a functional role in signaling under physiological conditions (Baldwin et al., 2005).

Although studies of the mechanisms involved in regulating extracellular adenosine continue to accumulate, questions remain that better understood enzymes and proteins, including ENT1 and 2, are not able to fully answer. As such, alternative and initially ignored proteins, such as ENT3, may be more involved than first thought. Expression on the lysosomal and mitochondrial membranes would enable ENT3 to directly modulate cytosolic adenosine concentrations; degradation processes within lysosomes are a potential source of adenosine, which could then be released to the cytosol. These direct sources of intracellular adenosine, transported by hENT3, may become available for release to the extracellular matrix, via plasma membrane-located ENT1 and 2.

Alternatively, in some cell types, hENT3 may be expressed on the cell membrane and therefore could play roles similar to that of ENT1 and 2 in regulating extracellular adenosine. Additionally, as hENT3 has been demonstrated to have optimal activity at pH between 5.5 and 6.5 (Baldwin et al., 2005; Govindarajan et al., 2009), hENT3 expressed on the cell surface could be highly active in pathophysiological conditions, such as ischemia, in which extracellular pH decreases. Under such conditions, hENT3 could potentially contribute to the influx of extracellular adenosine, which would have two effects. First of all, the uptake of adenosine by ENT3 would terminate adenosine signaling; although the neuroprotective actions of adenosine via A_1 receptors contribute to cell survival in such conditions,

over activation of the same receptors could have detrimental effects and as such extracellular adenosine concentrations need to be strictly regulated (Dunwiddie and Masino, 2001; Picano and Abbracchio, 2000). Secondly, under such pathophysiological conditions, controlled ATP release may be compromised resulting in excessive ATP loss from cells; under such circumstances adenosine salvage via ENT3 may become important.

As mentioned previously, accumulating evidence has demonstrated adenosine can be released directly by exocytosis, a mechanism dependent both on action potentials and Ca^{+2} (Wall and Dale, 2008; Wall and Dale, 2013). Such a release mechanism indicates the need for adenosine to be stored, at least in part, in vesicles or granules within the cell until a specific stimulus provokes their fusion with the plasma membrane and subsequent release of adenosine into the extracellular space. Although such release mechanisms have been demonstrated using microelectrode biosensors, it remains unclear how adenosine is packed within vesicular carriers for storage; hENT3 could potentially be this missing link and should be explored further.

1.3.2.4. ENT4

hENT4, a 530-residue protein, was discovered by genome database analysis, as ENT3 was, after completion of the human genome project (Acimovic and Coe, 2002). Although ENT4 exhibits low sequence homology to the other ENT isoforms, preliminary studies have predicted ENT4 topology to be characteristic of other ENT members and Na^{+}-independent (Acimovic and Coe, 2002). In comparison to ENT1 and 2, ENT4 presents some unique properties.

Initially classified as a low-affinity adenosine transporter of the ENT family (Baldwin et al., 2004), a separate study identified it as plasma membrane monoamine transporter (PMAT) that was demonstrated to efficiently transport serotonin and dopamine and was found to have no interaction with nucleosides or nucleobases (Engel et al., 2004). These conflicting reports were later resolved as ENT4 nucleoside transport activity was discovered to be pH dependent; similarly to ENT3, adenosine transport was optimal at an acidic pH (Barnes et al., 2006). The effect of pH on transport of monoamines and other organic cations is still debated (Barnes et al., 2006; Zhou et al., 2010). Currently, ENT4 is classified as a dual nucleoside/organic cation transporter.

Tissue distribution studies of hENT4 have found it to be widely expressed with highest levels of expression in brain, skeletal muscle and heart, which in conjunction with the observed pH-dependent adenosine transport suggests ENT4 to be critical in pathophysiological conditions that alter the environmental pH, such as ischemia of the brain or heart (Barnes et al., 2006).

To date, very little is known about ENT4, in terms of both localisation and function. Although classified as a member of the ENT family, the low sequence homology (≈20%) and stark differences between ENT4 and the other ENT isoforms, including substrate specificity, may be good indicators that ENT4 is more involved in monoamine than purinergic signaling, however, adenosine influx by ENT4 may be important in pathophysiological conditions of low pH (e.g. stroke) (Zhou et al., 2010).

1.4 ENTs and Human Disorders

Studies have been conducted to identify links between ENTs and human diseases and although changes in ENT expression profile or protein level are suggested to be contributing factors to certain disease states only mutations of the hENT3 gene have been found directly responsible for human disorders. ENT1 and 2 have overlapping characteristics, both in terms of expression profile and activity, whereby a mutation in one could potentially be silenced by the other. As ENT3 does not share many of the same transporter properties as ENT1 and 2, it is possible that mutations within the ENT3 gene resulting in altered localisation or function would not be overcome by the presence of other ENT isoforms.

Recently, mutations in the SLC29A3 gene have been linked to autosomal-recessive genetic disorders in humans, such as H syndrome and pigmentary hypertrichosis and insulin-dependent diabetes mellitus (PHID), which will be described in detail below. It is interesting to note that these disorders are not due to one specific mutation of the SLC29A3 gene but multiple mutations have been identified as causal factors, with varying degrees of severity, suggesting a pleiotropic nature of such disorders. H syndrome and PHID syndrome are the most well-known syndromes associated with SLC29A3 mutations in humans although others have been identified including Faisalabad Histocytosis, Familial Rosai-Dorfman disease and dysosteosclerosis.

Alterations of the ENT3 gene sequence can elicit a variety of effects at the cellular level including changes to adenosine transport kinetics, mistrafficking and increased degradation and turnover rates (Kang et al., 2010). As a result of such gene mutations, patients often present with multiple clinical phenotypes, and varying degrees of severity. This is perhaps

not surprising as hENT3, considered a mitochondrial and lysosomal transporter, is involved in nucleoside salvaging pathways and

as such, gene mutations that alter endogenous hENT3 would have a systemic effect (Spiegel et al., 2010). Due to the lack of knowledge of hENT3, both the basis of development and the pathogenesis of such syndromes remains unknown.

1.4.1 H Syndrome

H syndrome is an autosomal recessive disorder that has been recently linked to mutations of the *SLC29A3* gene encoding the previously described hENT3 protein, a poorly understood nucleoside transporter. In terms of clinical phenotype, H syndrome, also identified as OMIN 612391, is primarily characterized by cutaneous hyperpigmentation (darkening of an area of skin), hypertrichosis (abnormal hair growth), histiocytosis (excessive number of histiocytes or macrophages), hearing loss and short stature (Huber-Ruano et al., 2012; Priya et al., 2010). This syndrome was identified by studying collections of case reports compiled from patients with similar, although not identical, symptoms; genotyping determined that all patients share the same multisystemic disorder. “H syndrome” was suggested to name the previously unnamed disorder as the majority of the principle defining characteristics begin with the letter ‘h’ (Molho-Pessach et al., 2008a).

As has been previously stated, the precise localisation of hENT3 remains undetermined. This being said, studies of patients with H syndrome may offer vital information to determine hENT3 localisation based on the effects of mutated and malfunctioning hENT3 protein. A number of the more common symptoms associated with H syndrome are linked to malfunction of the mitochondrial respiratory-chain, such as short stature, which supports

the current findings suggesting ENT3 to be a mitochondrial transporter (Govindarajan et al., 2009; Priya et al., 2010). Others reflect known lysosomal disorders which supports findings indicating ENT3 to be a lysosomal transporter involved in nucleoside salvaging pathways (Baldwin et al., 2005). However, as H syndrome is not characterized by the buildup of storage material, which would be highly indicative of lysosomal dysfunction, one could argue that lysosomes are not affected by SLC29A3 mutations that would disprove such studies (Kang et al., 2010)

Although multiple studies of H syndrome have been performed (de Jesus et al., 2013; Elbarbary et al., 2013; Farooq et al., 2012; Hiller et al., 2013; Kang et al., 2010; Molho-Pessach et al., 2008a; Priya et al., 2010), comparisons between them are difficult as there is not one sole mutation in the hENT3 gene that is responsible but numerous individual mutations have been identified that may be the causal factor of H syndrome. Of 11 families of Arab and Bulgarian origin, three *SLC29A3* gene mutations were identified, two missense mutations (c.1279G>A and c.1309G>A) and one deletion mutation (c.1045del) (Molho-Pessach et al., 2008b) but others have been identified including additional missense mutations (c.347T>G and c.1309G>A) and deletion mutation (c.940delT) (Cliffe et al., 2009). It is possible that the localisation of each mutation, and certainly more than those identified above may exist, dictates the clinical outcome by differently impacting the function, stability and/or localisation of hENT3. Due to the enormous variation in both symptoms and severity of symptoms in patients with H syndrome, it is evident that further studies of ENT3 are needed in order to fully understand the pathogenesis of such human disorders and both the physiological and pathophysiological roles of ENT3, although it should be noted that H syndrome may not be the best model for such studies due to the pleiotropic nature of

SLC29A3 mutations. The variety of hENT3 mutations contributes to misdiagnosis and under diagnosis of H syndrome.

1.4.2 PHID Syndrome

Recently described PHID syndrome is an autosomal, recessive genetic disorder identified in humans to be due to mutations within the SLC29A3 gene (Cliffe et al., 2009). Although PHID syndrome and H syndrome are allelic, often presenting overlapping clinical symptoms, there are some important differences (Cliffe et al., 2009). Primarily, PHID syndrome differs by the development of a syndromic form of insulin-dependent diabetes within the second or third decade of life which has not been found to develop in patients with H syndrome (Cliffe et al., 2009). PHID syndrome was determined to be caused by mutations in the SLC29A3 gene, encoding the hENT3 protein, a still poorly understood NT which is thought to be vital to nucleoside salvage pathways and perhaps other physiological processes.

Currently, five different mutations have been identified and linked to PHID syndrome, two encoding a truncated protein (c.940del, c.1330G>T) and three missense mutations (c.347T>G, c.1309G>A and c.1346C>G) and although these mutations have been clearly established as the causal factors in PHID syndrome the mechanism of development and the link to insulin signaling remains unknown (Cliffe et al., 2009; Kang et al., 2010). Although PHID syndrome and H syndrome share similar dermatological features, including areas of hyperpigmentation and hypertrichotic skin, there are important differences depending on the type of mutation, in-frame, out-of-frame, point mutations or multi-exon deletions, although it has been suggested that poorly understood differences in genetic background or

environmental effects could contribute to identical mutations resulting in different observed phenotypes (Cliffe et al., 2009).

Type 1 diabetes, characterized by the loss of insulin-producing pancreatic β-cells, can occur in conjunction with other syndromes. Studies have been conducted to elucidate the connection between ENT3 and the insulin signaling pathway; as insulin signaling regulates growth and proliferation pathways, ENT3 could potentially contribute to maintaining appropriate nucleoside levels required for cell growth (Cliffe et al., 2009). One group used *Drosophila melanogaster* as animal model to study the effects of ENT3 knockdown on the well characterized insulin signaling pathways within *Drosophila* and were the first to demonstrate the link between hENT3 mutations and diabetes mellitus (Cliffe et al., 2009*).*

1.5 Pharmacological Implications of ENTs

Nucleoside analog drugs (NADs) represent an important drug class that is used to treat human diseases such as cancers as well as viral and parasitic infections. NADs are predominantly hydrophilic in nature and as a result are unable to cross cell membranes without membrane transporter proteins, such as CNT and ENT isoforms, as they are nucleoside analogs and therefore closely resemble the endogenous substrates. Although NTs vary in their substrate selectivity and their activity in transporting such therapeutic agents. Once incorporated into the cell, NADs are subjected to metabolism by cell enzymes to form their active triphosphate derivatives, which may then be incorporated in place of endogenous nucleotides into DNA, inducing DNA chain termination and apoptosis. It is important to note that NAD activity and consequently the therapeutic benefit of NADs, is completely

dependent on the initial uptake by NTs. Further knowledge of the endogenous expression profile, in addition to changes to expression in disease states, of specific NT subtypes will greatly impact the therapeutic outcome.

It has been previously demonstrated that metabolic and physiological conditions of stress stimulate increased extracellular adenosine concentrations. The resulting activation of corresponding adenosine receptors initiates the neuromodulatory actions and neuroprotective effects of adenosine within the CNS which have been well documented. Such signaling pathways are dependent on those mechanisms that regulate extracellular adenosine concentration, which includes the ENT family of bidirectional adenosine transporters. As such, therapeutic agents that target ENT isoforms represent important novel strategies by which adenosine concentrations could be modulated. Furthermore, the identification and impact of single nucleotide polymorphisms (SNPs) within the ENT family coding sequences could improve drug dosing and individual therapeutic benefit (Damaraju et al., 2003).

1.5.1 NADs- Anticancer Agents

The majority of studies on NTs have focused on the better known ENT family members, ENT1 and 2, to explore the roles of such transporters in NAD efficacy. As hENT1 is the best characterized ENT isoform, the majority of studies have been performed investigating the link between hENT1 expression variations and patient response to anticancer agents.

For example, one group studied the link between hENT1 in primary breast cancer and concluded that hENT1 protein deficiency conferred a high-level of resistance to drug cytotoxicity, which resulted in ineffective treatment (Mackey et al., 2002). Based on their

findings, they suggested immunodetection of hENT1 in biopsy samples could prove a useful predictive tool enabling improved drug dosing (Mackey et al., 2002). A similar study was conducted by a second group, Nishio et al, which looked at the direct effects of hENT2 on a widely used nucleoside pyrimidine analog, gemcitabine (Nishio et al., 2011). Gemcitabine is considered to be one of the most effective therapeutic agents in advanced stages of pancreatic cancer, however, cellular resistance is known to develop. The disruption of ENT2 localisation on the plasma membrane, and the resulting decreased uptake and activation of gemcitabine, contributed to resistance (Nishio et al., 2011).

Numerous studies of anticancer and antiviral agents have been conducted and treatment with such therapeutics, including zidovudine, fialuridine and gemcitabine, often induced mitochondrial toxicity in various tissues such as liver and pancreas (Kohler and Lewis, 2007; McKenzie et al., 1995). Evidence of mitochondrial toxicity suggests an endogenous mechanism by which NADs are taken-up into the mitochondria; as ENT3 is thought to be expressed on mitochondrial membranes, it could represent a potential mechanism by which NADs accumulate within mitochondria disrupting normal organelle function (Govindarajan et al., 2009). Alternatively, ENT3 is thought to be a lysosomal transporter, which could potentially result in the accumulation and increased degradation of NADs within lysosomes; increased ENT3 activity would alter drug properties (Zhang et al., 2007). Subcellular localisation and substrate specificity of ENT3 will directly impact NAD therapy, in terms of effectiveness and potential toxic effects, although it may remain difficult to assess the effects of ENT3 in terms of NAD therapy as localisation has been suggested to be cell-type dependent and therefore would affect cells differently (Govindarajan et al., 2009).

1.5.2 NADs- Antiviral Agents

Viruses infect millions of people worldwide. For many viruses no vaccines are currently available and treatment regimens that have been established to treat viral infections are met with mixed success. Many questions remain as to the factors that determine treatment response.

Although the precise antiviral mechanism is unknown, ribavirin is currently used to treat hepatitis C (Ibarra and Pfeiffer, 2009). Ribavirin is a NAD and therefore is dependent on cellular uptake by NTs; within the cytosol ribavirin is activated by host enzymes and disrupts viral mechanisms. Known to be an effective antiviral in many patients, drug resistance has developed in numerous cases although no clear mutations have been identified to cause this resistance (Ibarra and Pfeiffer, 2009). In light of this, studies of the ENT and CNT families have been performed to assess what, if any, effect NTs had in drug resistance of ribavirin. It was demonstrated that ENT1 was critical in ribavirin uptake and by blocking ENT1 activity by NBMPR, ribavirin resistance developed suggesting cellular response mechanisms, which down regulate ENT1 under prolonged ribavirin exposure and thereby limit amount of active intracellular ribavirin (Ibarra and Pfeiffer, 2009). This illustrates the importance of NTs in terms of therapeutics and the challenges associated with resistance mechanisms.

There are a number of known antiviral agents that are ENT substrates, such as zidovudine which is used in HIV infections. The therapeutic outcome of such NADs will be in-

fluenced by the localisation and abundance of ENT isoforms. Treatment strategies and patient outcomes could be improved by further understanding of the ENT family, which would enable optimal dosing.

1.5.3 ENT Inhibitors

Over the years, many attempts have been made to develop adenosine analogs. This is in response to studies demonstrating the signaling properties of adenosine, including anticonvulsant effects and neuroprotective properties. Unfortunately attempts to mimic a particular effect of adenosine, in a specific manner, have been met with little success for a variety of reasons. Adenosine is rapidly cleared from the extracellular space either through the action of uptake transporters or, in some cases, is quickly broken down by extracellular enzymes to terminate signaling cascades. Utilizing synthetic adenosine receptor agonists is not ideal as they can have serious, widespread negative side effects due to the ubiquitous expression of adenosine receptors these include hypotension, bradycardia and sedation. As an alternative strategy, there exists high potential therapeutic implications in targeting the ENT family (Chen et al., 2007; Choi et al., 2004; Keil and Delander, 1995; Parkinson et al., 2000) as inhibition of ENTs would maintain a high extracellular adenosine concentration for an extended period of time, resulting in increased adenosine signaling.

A number of ENT inhibitors are currently approved for clinical use, including dilazep and dipyridamole, two coronary vasodilators, which are perhaps the most well-known ENT inhibitors. They have been shown to induce vasodilatory actions in multiple mammalian species although the potencies for ENT1 and 2 vary among species (Griffith and Jarvis,

1996). A novel study has characterized ticagrelor, a known $P2Y_{12}$ receptor antagonist, currently approved as a prophylactic therapy to reduce the rate of mortality from vascular causes (Armstrong et al., 2014). Surprisingly, ticagrelor was found to have effects on extracellular adenosine concentrations by inhibiting adenosine uptake via inhibition of ENT1; it was proposed that the resulting increased signaling via adenosine receptors could explain $P2Y_{12}$ independent beneficial effects of this drug (Armstrong et al., 2014).

Similarly to concerns that were first observed with adenosine analogs

Although the therapeutic potential of ENTs are of great interest concerns, similar to those surrounding the use of adenosine analogs, remain. As ENTs are found to be expressed in numerous tissues and cell types throughout the body therapeutic agents designed to target members of the ENT family could induce widespread undesirable systemic effects. In order to overcome these concerns, further studies are needed as subtle differences in expression profiles, localisation and substrate selectivity could contribute to improve drug design and improve patient outcomes.

Chapter 2

Rationale & Objectives

2.1 Rationale

By activating cell surface GPCR, adenosine initiates intracellular signaling cascades within brain that have been well characterized. Depending on the type of adenosine receptor and the associated G-protein adenosine can induce a variety of effects within the CNS including anticonvulsant actions, regulation of sleep/arousal states, regulation of pain signal transmission and neuroprotection. Although these signaling pathways have been well characterized, the mechanisms that govern extracellular adenosine concentrations are far less understood. As all known adenosine receptors are cell surface receptors, activation of any signaling cascade depends on the availability of adenosine within the extracellular space to bind to corresponding receptors. The balance between adenosine uptake and release is critical to normal cellular processes and must be strictly controlled.

Nucleoside transporters are a family of membrane bound transporters that enable hydrophilic nucleosides and nucleobases, such as adenosine, to cross cell membranes, which they otherwise could not do. One family of NTs are the ENT family, comprised of four

subtypes (ENT1-4). ENT1 and 2 were first discovered and, due to the availability of appropriate molecular tools, they have been best characterized to date whereas ENT3 and ENT4, almost 15 years after their discovery, remain poorly understood.

Although ENT1 and 2 are currently considered to be the primary mechanisms regulating extracellular adenosine concentration (Baldwin et al., 2004; Griffiths et al., 1997; Jennings et al., 2001; Ward et al., 2000) they are unable to fully explain observed release phenomenon *in vivo*. In order to further our understanding of adenosine signalling cascades, attention has turned to lesser known proteins, such as ENT3 and 4, to determine what role, if any, such proteins play in regulating adenosine concentrations.

As studies of ENT3 are limited (Baldwin et al., 2005; Govindarajan et al., 2009; Hsu et al., 2012; Kang et al., 2010), and studies of ENT3 within brain are even more so (Li et al., 2013; Lu et al., 2004), this project consists of investigating ENT3 expression and abundance within brain and confirming intracellular localisation, as has been suggested in current studies (Baldwin et al., 2005; Govindarajan et al., 2009; Hsu et al., 2012). Furthermore, we hope to elucidate the functional role of ENT3, specifically in terms of adenosine transport and potential involvement in signaling pathways.

2.2 Objectives

2.2.1 Validate Commercial AntiENT3 Antibody

Due to the lack of experimental data verifying commercial antiENT3 antibodies, we will create a flag-tagged mENT3 protein using recombinant technology that will be transfected

into cells enabling us to test any commercial antibody, compared to an antibody specific to the flag epitope, for specificity to the ENT3 protein.

2.2.2 Determine ENT3 localisation within brain

To assess localisation and expression of mENT3 within brain, mice will be dissected and the cortex, cerebellum, striatum and hippocampus will be harvested. To determine mENT3 mRNA expression, mRNA will be isolated from each brain region to synthesize cDNA and probed with a primer targeting the mENT3 gene sequence. In addition, tissue protein will be homogenized and subjected to western blot analysis to assess relative protein expression throughout brain. Furthermore, primary cell cultures, neurons, astrocytes and microglia, will be assessed for both mENT3 mRNA expression and protein expression similarly.

2.2.3 Determine subcellular ENT3 localisation

To determine subcellular localisation of mENT3, primary cell cultures of neurons and astrocytes will be costained with an antibody targeting ENT3 and a cellular marker, NeuN or GFAP respectively; cells will be imaged by fluorescence microscopy. In addition, differential centrifugation will be performed using mouse brain tissue samples, by which four fractions will be collected, nuclear, mitochondrial, plasma membrane and cytoplasmic, and tested for ENT3 expression by western blot analysis.

2.2.4 Determine ENT3 activity in nucleoside transport

To investigate ENT3 function, a stable transfected cell line overexpressing ENT3 protein will be created. By initially incubating cells with [^{3}H]adenine, to tritiate intracellular ATP, purine release from WT and transfected cells activity will be compared under a number of experimental conditions. Total purine release will be counted by measuring total extracellular and intracellular purines by scintillation spectroscopy and release of the individual purines adenosine, inosine and hypoxanthine will be determined following a thin layer chromatography (TLC) separation procedure.

Chapter 3

Methods

Unless otherwise indicated, tissues and cultured cells were homogenized in NP-40 buffer containing 150 mM sodium chloride, 1% NP-40 (Sigma-Aldrich), 50mM Tris (Fisher Scientific). A pH of 8.0 was achieved with addition of HCl. NP-40 buffer was stored at 4°C for up to 8 weeks. Immediately prior to using, PMSF (Sigma-Aldrich; P-7626) was added for a final concentration of 0.3 mM and a protease inhibitor cocktail tablet, a complete mini tablet from Roche Applied Science (1836153) was added to 10 mL NP-40 buffer.

3.1 Creation of pIRES-puro-Flag-mENT3 plasmid

The pIRES-puro-Flag plasmid, containing the gene sequences conferring resistance to ampicillin and puromycin, was generously donated by Dr. Mike Jackson (University of Manitoba, Winnipeg, Manitoba).

3.1.1 Selection of source of mouse ENT3 cDNA template

To verify astrocytes as an acceptable template source of the mouse ENT3 sequence, previously prepared cDNA from mouse cortical astrocytes was assessed for the presence of mENT3 cDNA, using a primer pair targeting the ENT3 gene, designed to amplify a band size of 1.4Kb. In addition, template cDNA was probed with a control primer targeting the mouse GAPDH gene designed to amplify a band size of 188bp. PCR was performed using PuReTaq Ready-To-Go beads (GE Healthcare Illustra; 27-9557-02) in a 25 µL reaction consisting of template cDNA and 5µM of appropriate forward and reverse primers, completed with water. mENT3 primers were designed containing the appropriate restriction sites, AscI and Not1, to enable insertion of the gene sequence into pIRES-puro-Flag plasmid.

mENT3- NM_023596.3 (1.4Kb):

AscI-Fw: AGGCGCGCCAGCCTTTGCCTCTGAGGACAATGTATA

Not1Rv: ATTAGCGGCCGCCTAGATAAAGTGTTCAAGCAGGGC

All PCR reactions were performed using a PTC-100 Programmable Thermal Controller (MJ Research, Inc) and the following parameters: initial denaturation was performed at 95°C for 45 sec followed by 30 cycles consisting of denaturation at 95°C for 45 sec, annealing at 70°C for 45 sec and elongation at 72°C for 2 mins with a final elongation step at 72°C for 10 mins. Samples were held at 4°C until collected.

PCR products were analyzed by electrophoresis; samples were run on a 1% agarose gel (Promega; V3121) containing 0.001% v/v ethidium bromide (Sigma-Aldrich; E-1510) enabling visualization of DNA bands under exposure to UV light using Kodak Gel Logic 100

Imaging System. Images were captured using Kodak ID v.3.6.3 (Scientific Imaging Systems; New Haven, CT, US).

3.1.2 Cloning of mENT3 PCR Product

To ensure sufficient mENT3 cDNA would be harvested, multiple PCR reactions were performed using previously verified mouse cortical astrocyte cDNA as the template source for the mENT3 cDNA sequence. PCR reactions were performed as previously described, in section 3.1.1.

To harvest mENT3 cDNA, samples were separated on an agarose gel, using fresh TAE buffer to maximize purity of cDNA samples. Bands of the appropriate size of 1.4Kb, were excised from the agarose gel using a sharp knife and were purified using GenElute Gel Extraction Kit (Sigma-Aldrich; Na1111-1KT) and following the manufacturer's protocol. To ensure correct mENT3 gene insertion with the pIRES-puro-Flag plasmid, appropriate primers were designed including complimentary restriction enzyme sites of AscI and Not1, to align the gene of interest with the flag-tag sequence. This enabled correct ligation resulting in a fusion protein of mENT3 protein with flag epitope and no shift in codons. Primer sequences are provided below, with the restriction enzyme sequence indicated underlined and the precise site of cut between the two bases indicated in bold.

mENT3- NM_023596.3

mENT3-AscI-Fw: AG**GC**GCGCCAGCCTTTGCCTCTGAGGACAATGTATA

mENT3-NotI-Rv: ATTAG**CG**GCCGCCTAGATAAAGTGTTCAAGCAGGGC

3.1.3 Ligation

Ligation was performed in two steps. To begin with, harvested PCR products and pIRES-puro-Flag plasmid were digested in separate reactions using Asc1 and Not1 restriction enzymes (New England Biolabs) for 3 hours at 37°C. Asc1 digestion was completed using NE CutSmart buffer (50 mM potassium acetate, 20 mM Tris-acetate, 10 mM magnesium acetate and 100 µg/mL BSA); Not1 digestion required NE buffer 3.1 (100 mM NaCl (Fisher Scientific), 50 mM Tris-HCl, 10 mM $MgCl_2$ (Fisher Scientific) and 100 µg/mL BSA). In addition the pIRES-puro-Flag plasmid was treated with calf intestinal alkaline phosphatase (CIP) (New England Biolabs; M0290), to minimize spontaneous religation of the plasmid. CIP was added to the plasmid solution for the final hour of incubation at 37°C. Both the digested PCR products, known as the insert, and the digested plasmid were separately purified using GenElute Gel Extraction Kit (Sigma-Aldrich) following the manufacturer's protocol. To determine DNA concentrations, samples were exposed to UV light at 260 nm using an Eppendorf Biophotometer Plus spectrophotometer which detects the amount of light passing through the sample; DNA concentration was determined based on the conversion factor of an optical density of 1 corresponds to 50 µg of DNA.

The second step of ligation consisted of combining the DNA insert with the digested plasmid DNA in appropriate conditions. Ligation was performed at a molar ratio of 3 insert to 1 plasmid as determined with Promega Biomath calculator using the following formula:

$$\frac{\text{(Kb of insert)}}{\text{(Kb of plasmid)}} \times 100\text{ng of plasmid} = \text{ng of insert}$$

This formula gives the amount of insert required for a 1:1 ratio; this was multiplied by three to calculate the amount of insert needed for a 3:1 ratio. The ligation mixture consisted of the digested insert and the digested plasmid combined with 1x ligase buffer and T4 DNA ligase (New England Biolabs; M0202), selected due to its high fidelity, completed to a final volume of 10µL with water. The total mixture was incubated for one hour at RT. Following ligation, pIRES-puro-Flag-mENT3 plasmid, known as the ligate, was used for transformation and the excess was stored at -80°C.

3.1.4 Transformation

All agitation was maintained at 225 rpm using a Max^{Q} Mini 4450 shaker (Barnstead Lab-Line) unless otherwise indicated.

50 µL XL10 Gold Ultracompetent *Escherichia coli* (Strategene; 200314) was thawed on ice and allocated to a prechilled BD Falcon polypropylene round-bottom transformation tube and combined with 2 µL β-mercaptoethanol, known to improve transformation efficiency. The reaction was incubated on ice for 10 mins, during which the solution was mixed by hand every two mins. 3 µL of ligate was added to the *E.coli* mixture and incubated for 30 mins. Cells were heat-shocked at 42°C for exactly 30 sec and put directly on ice for 2 mins. Prewarmed SOC medium (2% w/v tryptone, 0.5% yeast, 8.56 mM NaCl, 1 M $MgCl_2$, 1 M $MgSO_4$ and 2 M glucose) was added to the cell solution and cells recovered at 37°C for one hour with constant shaking.

Transformants, *E.coli* cells that had incorporated the plasmid DNA during transfection, were selected using LB agar plates containing 100 mg/mL ampicillin (Bioshop Canada). LB plates were prepared by combining 171 mM NaCl 1% w/v tryptone, 0.5%

w/v yeast, 2% w/v agar. A pH of 7 was obtained using NaOH. The mixture was autoclaved and allowed to cool to RT before adding ampicillin to a final concentration of 100 mg/mL. Approximately 30 mL of LB agar medium was immediately added to 100 mm dishes and allowed to set; LB agar plates were used directly or were sealed and stored at 4°C for up to two weeks. 50 µL of bacterial suspension was plated and allowed to dry before placing plates in a 37°C incubator overnight. Colonies that grew on the LB plates were expected to have successfully acquired the plasmid DNA which contains an ampicillin-resistance gene; bacteria that did not incorporate the plasmid would not be able to survive in the presence of ampicillin.

Individual transformed *E.coli* colonies from LB plates were transferred to separate BD Falcon tubes containing 2 mL LB broth with ampicillin. Selected transformants were grown overnight at 37°C with agitation, these cultures are known as starter cultures. The following day plasmid DNA from the *E.coli* cultures was harvested using Gibco Concert Rapid Plasmid Maxiprep kit (Qiagen; 12162) altered slightly to accommodate the smaller volume of the starter cultures. The modified protocol is detailed below.

1 mL of LB medium from each starter culture was transferred to an Eppendorf tube and centrifuged for 5 mins at 12,600 rpm (14,800xg) at 4°C. The supernatant was removed and 200 µL resuspension buffer (50 mM Tris pH 8, 10 mM EDTA and 100 µg/mL RNase A) was added and the sample was vortexed to completely resuspend the pellet. 200 µL lysis buffer (200 mM NaOH, 1% w/v SDS purchased from Bio-Rad; 161-0301) was added and the sample was mixed by hand and incubated for 5 mins at RT. 200 µL neutralization buffer (3 M potassium acetate, pH 5.5) was added and mixed thoroughly. Samples were incubated for 15 mins on ice and centrifuged for 10 mins at 12,600 rpm at 4°C. The supernatant was

transferred to a fresh Eppendorf tube and 900 µL 95% cold ethanol was added. The solution was incubated on ice for an additional 10 mins before samples were centrifuged for 20 mins at 12,600 rpm at 4°C. The supernatant was discarded and the pellet was washed once by centrifuging samples with 70% ethanol for 10 mins at 12,600 rpm at 4°C. The wash supernatant was removed and the pellet was left to air dry for approximately 10 mins before resuspending the pellet in DNAse and RNAse free water (Invitrogen; 10977-015). The collected pellet contained the pIRES-puro-Flag-mENT3 plasmid.

As an initial means of verifying the incorporated plasmid in transformants for the mENT3 gene insert, collected plasmid DNA was subjected to a diagnostic digestion. NheI was chosen based on the restriction enzyme sites of pIRES-puro-Flag-mENT3; ligation of mENT3 gene insert within the plasmid contains three digestion sites resulting in three distinct bands of 226bp, 771bp and 5.6Kb following digestion whereby an empty plasmid would contain only one NheI site resulting in linearization of the plasmid and one sole band. Digestion by NheI (New England Biolabs) was performed for one hour at 37°C in 20 µL reactions containing NE buffer #4, 1x BSA, 5 µL ligate and NheI, completed in water. Following incubation, the digested ligate was analyzed by electrophoresis on an agarose gel and visualized as previously described.

A midi prep, consisting of 50 mL of LB broth containing ampicillin, was inoculated with 50 µL of starter culture selected based on the success of the previously described digestion of Nhe1. The midi prep was grown overnight at 37°C with shaking. The following day total bacterial suspension was centrifuged at 4,500 rpm for 10 mins at 4°C to collect all *E.coli* cells; plasmid DNA was harvested and purified using GenElute HP Plasmid Mi-

diprep Kit (Sigma-Aldrich; Na0200-1KT) following the manufacturer's protocol. To confirm plasmid samples were sequenced at the Manitoba Institute of Cell Biology using the primers shown below.

CMV-F: FP 5' TATTAGGACAAGGCTGGTGGGCAC
mENT3 (419-F): FP 5' GTGTTCTGGCCTCACTGTCC
mENT3 (911-F): FP 5' TGGACCCATCCTGAAGAAG

3.2 Transfection of pIRES-puro-Flag-mENT3 Plasmid

3.2.1 Culture of HEK293T Cells

HEK 293T cells were a generous gift from Dr. Mike Jackson (University of Manitoba, Winnipeg, Manitoba).

Cells were grown in high glucose DMEM (Invitrogen) containing 10% FBS (Life Technologies; 26140079) and maintained in a humidified 37°C incubator aerated with 95% air/5% CO_2. Cells were passaged at 90% confluence and were used until passage number 50.

One day prior to transfection cell media was removed and cells were washed with sterile PBS buffe**r** (145 mM NaCl, 3.8 mM NaH_2PO_4, 6.7 mM Na_2HPO_4). Cells were detached with trypsin-EDTA (0.25%; 1 mM) (Life Technologies; 25200-056) at RT for 1 min and subcultured in fresh DMEM (10% FBS) in 100 mm culture dishes allowing cells to be 60-70% confluent on day of transfection.

3.2.2 Transfection

Stable transfections were performed using jetPRIME DNA and siRNA transfection reagent (VWR International; CA89129-922). 5 µg of plasmid DNA was combined with 500 µL jetPRIME buffer and vortexed to mix completely. 12.5 µL jetPRIME reagent was added to the solution, mixed thoroughly and incubated for 10 mins at RT. The transfection solution was added in drops to culture dish and mixed by gently rocking the culture dish by hand. Cells were returned to the incubator. Four hours following transfection, total cell media was removed and fresh media was added. Two days following transfection, successfully transformed cells were selected with puromycin (InvivoGen; ant-pr-1) which was added to fresh media and maintained at 2 µg/mL. Cells were allowed to grow for a minimum of fourteen days before being lysed and harvested for experiments. Transfected cells were cultured continually in media containing 2 µg/mL of puromycin.

3.2.3 Validation of AntiENT3 Antibody

WT and transfected HEK293T cells were grown until 90% confluent in T-75 flasks. Working on ice, cell media was removed and cells were washed gently with 5 mL PBS to remove any remaining media. 600 µL of prechilled NP-40 lysis buffer was added directly to the culture dish and cells were harvested. Total cell suspension was incubated for 30 mins at 4°C with constant agitation and centrifuged at 13,000 rpm for 30 mins at 4°C. The supernatant was collected and the pellet was discarded. Protein concentration was measured as described in section 2.6.2.

To prepare samples for electrophoresis, Laemmli loading buffer (Sigma Aldrich; S-3401) was added to 40 µg of cell protein and samples were denatured by heating for 15 mins at 42°C before loading onto a 10% polyacrylamide gel and run at 150V. Separated protein samples were transferred to Immuno-blot PVDF membrane (Bio-Rad Laboratories; 162-0177) using Bio-Rad Trans-Blot SD Semi-Dry Electrophoretic Transfer Cell (Bio-Rad Laboratories, Mississauga, Ontario); transfer was maintained at 15V for 2 h.

Following transfer, the gel was stained with approximately 20 mL Bio-Safe Coomassie Blue (Bio-Rad; 161-0786) for one hour at RT to evaluate the electrophoresis. The membrane was incubated in 10 mL blocking buffer consisting of 5% w/v skim milk in Tris-buffered saline with tween (TBS-T) (50 mM Tris-HCl, 150 mM NaCl pH 7.5, 0.05% Tween-20 purchased from Fisher Scientific; BP-337) for 60 mins at RT with constant agitation. Membranes were incubated in primary antibody, diluted in blocking buffer, overnight at 4°C with constant shaking. The primary antibodies used were 1:200 dilution of ENT3(N-20) (Santa Cruz Biotechnology; sc-48150) and 1:1,000 ANTI-FLAG M2-Peroxidase (Sigma-Aldrich; A8592). The following day membranes were washed three times for 10 mins each at RT in TBS-T before incubating the membrane for 60 mins at RT in the appropriate secondary antibody. The secondary antibody corresponding to ENT3(N-20) was donkey anti-goat IgG-HRP (Santa Cruz Biotechnologies; sc-2020) diluted to 1:5,000 in blocking buffer. ANTI-FLAG M2 Peroxidase is conjugated to HRP and does not require a secondary antibody for visualization.

Following incubation in appropriate secondary antibody, membranes were washed as previously described and bands were visualized by incubating membranes for 60 sec in Clarity Western Blot Substrate (Bio-Rad; 170-5060). The excess Clarity Blot Substrate

was removed and membranes were immediately visualized using Bio-Rad ChemiDoc MP. Images were captured using ImageLab 5.1 Beta Build 1 software. To determine specificity of commercial antibody, band sizes of samples using ENT3(N-20) were compared to those as identified using ANTI-FLAG M2 peroxidase, which is specific to the plasmid flag-tag.

3.3 Characterization of HEK293T Cells

3.3.1 Reverse Transcriptase Polymerase Chain Reaction (Rt-PCR)

3.3.1.1. RNA Isolation

To minimize the risk of contamination of samples, sterilized pipet tips, microcentrifuge tubes, cell scrapers, needles and syringes were used.

WT and transfected HEK 293T cells were grown to 90% confluent on T-75 flasks. Working on ice, cell media was removed and cells were washed gently with PBS. TRIzol reagent (Invitrogen Life Technologies; 15596026) was added directly to flask, cells were harvested and the total cell lysate was transferred to Eppendorf tubes. Cell lysate was incubated in TRIzol reagent for 5 mins at RT to ensure the complete dissociation of nucleoprotein complexes. 0.2 mL of chloroform was added per 1 mL of TRIzol reagent and samples were mixed by hand, Samples were incubated for 2 mins at RT and centrifuged at 12,000 rpm (14,800 x g) for 15 mins at 4°C. After the initial spin, the total cell lysate separates into three phases, for RNA isolation the top aqueous phase is transferred to a new

Eppendorf without disturbing the interphase. 0.5 mL isopropyl alcohol was added per 1 mL of TRIzol reagent, to precipitate RNA, samples were mixed by hand and incubated for 10 mins at RT. Samples were centrifuged at 12,000 rpm (14,800 x g) for 15 mins at 4°C and the supernatant was discarded. The RNA pellet was washed with 1 mL 75% ethanol per 1 mL of TRIzol reagent and vortexed. Samples were centrifuged a final time at 7,500 rpm (8,800 x g) for 10 mins at 4°C and the supernatant was discarded; samples were allowed to air dry for approximately 10 mins. Pelleted RNA samples were resuspended in ultrapure distilled water (Invitrogen; 10977-015) and heated for 10 mins at 55°C to maximize RNA resuspension. The concentrations of RNA samples were determined using Eppendorf BioPhotometer Plus spectophotometer to measure the absorbance at 260 nm; based on the optical density, RNA sample concentration was calculated using a conversion factor of 1:40 µg/mL of RNA.

Isolated RNA was immediately subjected to Rt to preserve the integrity of samples.

3.3.1.2. Rt: Reverse Transcription

All work was performed in a PCR workstation (Fisher Scientific) and required lab equipment was sterilized and sterile filter pipet tips were used to minimize contamination of samples. Water used for all reactions was ultrapure distilled DNAse and RNAse free water (Invitrogen; 10977-015).

Rt reactions were performed in two steps, using a Minicycler (MJ Research; Fisher Scientific). To begin, each Rt reaction combined 2 µg of total RNA with 50 µM Oligo$(dT)_{12\text{-}18}$ primer (Invitrogen; 18418-012) in a final volume of 12 µL in water. Samples

were heated to 70°C for 3 mins to denature the RNA and then placed directly on ice. The second step consisted of combining the remaining Rt reaction components, First Strand Synthesis Buffer, 2.5 mM dNTP mix and M-MLV Reverse Transcriptase (Ambion Life Technologies; AM2043), to a final volume of 20 µL. The solution was incubated for 60 mins at 42°C followed by 10 mins incubation at 92°C to inactivate the M-MLV Reverse Transcriptase. The completed Rt reaction, synthesized sample cDNA, was stored at -20°C until needed.

3.3.1.3. PCR: Polymerase Chain Reaction

All PCR reactions were performed using PuReTaq Ready-To-Go Beads whereby 1 µL previously prepared cDNA, protocol described above, was used for each PCR reaction combined with 200 nM primers and water for a final reaction volume of 25 µL. To characterize HEK293T cells, WT and transfected, sample cDNA was combined with the following primers:

Human ENT1- NM_001078176.2 (1227/1453): 227bp
FP 5’ TAT TCA TGT GGC CTG GGA AG
RP 5’ AGC TGG CTT CAC TTT CTT GG

Human ENT2- NM_006718528.1 (479/674): 196bp
FP 5’ CCT ACA GCA CCC TCT TCC TC
RP 5’ AGG TAG TAG CGG GCA AAC TT

Human ENT3- NM_018344.5 (542/730): 188bp
FP 5’ TCT TCA GCA GCA GCA TCT ACG
RP 5’ AGA GCA CGA GGA AGA CAG TGG

Human ENT4- NM_001040661.1 (241/444): 203bp
FP 5’ TCACCTTCGACAGTCACCAG
RP 5’ AGTCCACGTCCGTGATGAAG

Mouse ENT3- NM_023596.3**:** 245bp

FP 5’ CCC TCC CTG CTG TTC CTG GT

RP 5’ CAT GGG GAA GGA GCC TGT GA

PCR reactions were placed in a PTC-100 Programmable Thermal Controller (Fisher Scientific) and a PCR program with progressively decreasing annealing temperatures, identified as Slow-down, was used (Bachmann et al., 2003). Slow-down consists of 48 cycles with 30 sec at 94°C, 30 sec at temperatures that gradually decrease from 70°C to 53°C by lowering the temperature by 1°C every three cycles and 40 sec at 72°C. Once attaining 53°C annealing temperature, the reaction is subjected to 15 additional cycles of 30 sec at 94°C, 30 sec at 58°C and 40 sec at 72°C. A final elongation step consists of 10 mins at 72°C after which samples were maintained at -9°C (Bachmann et al., 2003).

PCR products were analyzed as previously described in Section 3.1.1.

3.3.2 Real Time Polymerase Chain Reaction (qPCR)

LuminoCt SYBR Green qPCR ReadyMix (Sigma-Aldrich; 060M6173) was used to perform all qPCR reactions using previously prepared cDNA. Individual qPCR reaction mix contained 2X LuminoCt SYBR Green qPCR ReadyMix, 25 µM forward primer, 25 µM reverse primer and the template cDNA; the reaction was completed with water to a final volume of 25 µL per reaction. The final reaction mix was loaded into a 96 well plate and reactions were performed in triplicate. As described by the manufacturer’s protocol, the following cycling parameters were used: initial denaturation at 95°C for 20 sec and 40 cycles of denaturation at 95°C for 3 sec and lastly an annealing/extension phase at 60°C for 15 sec this was followed by 5 mins at 68°C, 15 sec at 95°C and 15 sec at 60°C before

samples were slowly brought to 95°C over 20 mins and then held at this final temperature for 15 sec. All qPCR reactions were performed using a Mastercycler RealPlex^2 (Eppendorf) and results were analysed using the Mastercycler Ep RealPlex version 1.5.

To characterize and compare WT and transfected HEK293T cells, sample cDNA was amplified with the human ENT3 and ENT4 and mouse ENT3 primers listed in Section 2.3.1.3. Additional primers were:

Human ENT1- NM_001078176.2 (312/488): 177bp
FP 5' TGT CCC AGA ATG TGT CCT TG
RP 5' GAT GCA GGA AGG AGT TGA GG
Human ENT2- NM_006718528.1 (663/768): 106bp
FP 5' CCG CTA CTA CCT GGC CAA TA
RP 5' CTG GGG ACT ACT GGG AAT CC

3.4 Primary Cell Culture

Mouse astrocytes and microglia were generously donated by Dr. Tiina Kauppinen (University of Manitoba, Winnipeg, Manitoba). Dissection of pups and preparation of enriched astrocyte cultures and microglia cultures were performed by Gary Odero. Subsequent maintenance of astrocyte cultures was a cooperative effort between Gary and me.

Mouse cortical neurons were generously donated by Dr. Chris Anderson (University of Manitoba, Winnipeg, Manitoba). Culture dishes, mouse dissections and initial neuron preparations were performed by Dr. Ping Lu. Subsequent maintenance of neuronal cultures was my responsibility. Mouse hippocampal neurons were generously donated by Dr. Mike Jackson (University of Manitoba, Winnipeg, Manitoba). Dissections were performed by Dr. Yu-Feng Xie and neurons were maintained in culture by Natalie Lavine.

3.4.1 Astrocytes

24-72 hours after birth, CD1 mice pups were euthanized, brains were removed, cerebral cortex was dissected and mixed cell populations were maintained in culture. Dissection media contained HEPES (Fisher Scientific), 1% penicillin (Fisher Scientific; BP914-100) and 1% streptomycin (Fisher Scientific; BP910-50) in HBSS. Cells were cultured in T75 flasks, in media consisting of MEM, 10% FBS, 2mM L-glutamine (Life Technologies; 21051-024) and 1% streptomycin. When cultures achieved 90-95% confluence, approximately 5-7 days in vitro, microglial cells were removed by vigorously shaking the flask horizontally by hand (for 5-10 sec) and immediately transferring the cell medium containing dislodged microglia to a new flask. Cells in the original flask were considered an enriched astrocyte culture and washed with fresh MEM medium then treated with 0.5% trypsin for 6 mins at 37°C. Prewarmed cell media was added to resuspend the cells and the cell suspension was replated on flasks or multi-well culture plates. Enriched astrocyte cultures were treated with 25 µM CA (Sigma-Aldrich; C1768) 5-7 days following dissection to inhibit microglia growth; CA kills dividing cells by forming complexes with topoisomerase I resulting in DNA fragmentation and cell death (Azuma et al., 2001). The following day total cell media was removed and replaced with MEM media containing 3% FBS. Astrocytes were maintained as confluent cultures containing CA for up to a month until use.

3.4.2 Microglia

24-72 hours after birth, CD1 mice pups were euthanized, brains were removed, cerebral cortex was dissected and mixed cell populations were maintained in culture. Dissection

media contained HEPES (Fisher Scientific), 1% penicillin (Fisher Scientific; BP914-100) and 1% streptomycin (Fisher Scientific; BP910-50) in HBSS. Cells were cultured in T75 flasks, in media consisting of MEM, 10% FBS, 2 mM L-glutamine (Life Technologies; 21051-024) and 1% streptomycin. When cultures achieved 90-95% confluence, approximately 5-7 days in vitro, microglial cells were removed by vigorously shaking the flask horizontally by hand (for 5-10 sec) and immediately transferring the cell medium containing dislodged microglia to a new flask. Microglia were maintained in supplemented MEM media for up to one month or until needed.

3.4.3 Neurons

3.4.3.1. Cortical Neurons

Prior to dissection, 24 well culture plates were pretreated to make the environment more conducive to neuronal attachment and growth. 0.5 mL of Poly-D-lysine was added to each well and incubated for 30 mins at RT. Poly-D-lysine solution was removed and plates were washed twice with sterile PBS and allowed to air dry. Plates were used directly or stored at 4°C for up to two weeks.

Neurons were harvested from CD1 mice, at E14 or E15, and suspended in neuronal basal media (Life Technologies; 21103-049) (5% FBS, streptomycin and L-glutamine). Cells were plated on pretreated 24 well plates. The following day all media was gently removed and replaced with fresh neurobasal media without FBS. The third day CA was added to each well to a final concentration of 2 µM. On the fourth day total cell media was

gently removed and replaced with fresh neurobasal media without FBS. On the seventh day following cell harvest, neurons were used for subsequent experiments.

3.4.3.2. Hippocampal Neurons

Prior to dissection MatTek coverslip dishes (MatTek Corporation; P35G-1.5-14C) were prepared for neuronal cultures by pretreating with 50µg/mL poly-D-Lysine (Sigma; P0899). 200µL of poly-D-lysine was added directly to the coverslip and incubated for 45 mins at RT before removing the poly-D-lysine solution and washing the coverslip twice with PBS. Coverslip dishes were then ready for neurons; coverslip dishes were always prepared fresh on day of dissection and used directly.

Time-pregnant CD1 mice were dissected at E17-18 and the hippocampi were removed and kept in PBS buffer on ice. Isolated hippocampi were broken down into smaller pieces using a scalpel at which point the PBS was removed and tissue samples were washed once with fresh PBS. The wash buffer was removed directly and samples were incubated with trypsin for 15 mins at 37°C before adding 1 mg/mL DNAsel and incubating for another 15 mins at 37°C. The total trypsin solution was then gently removed and replaced with MEM/20%FBS media and tissue samples were allowed to settle to the bottom of the tube after which the supernatant was removed gently without disturbing the pellet. To wash the settled tissue, fresh MEM/20%FBS media was added and once again the supernatant was removed. Tissue samples were titrated eight times in filter-sterile neurobasal media (Life Technologies; 21103-049) supplemented with B27 (Life Technologies; 17504-044) and L-glutamine (Life Technologies, GlutaMax; 35050-061) which was added to the tube. The samples were then left, allowing time for the larger tissue pieces to settle at the bottom of

the tube; the supernatant was transferred to a new tube containing fresh B27 supplemented neurobasal media, without disturbing any tissue which had settled at the bottom. The larger, left over pieces were resuspended in fresh B27 supplemented neurobasal by titrating gently eight more times. The larger pieces that had not been broken up were again allowed to settle at the bottom of the tube at which point the supernatant was added to the first collection. 250µL of the harvested cells was then seeded directly on to prepared coverslips and incubated for 30 mins before adding 2mL fresh supplemented neurobasal media to each dish.

Every 3-4 days approximately 1mL of cell media was removed and replaced with 1mL fresh B27 supplemented neurobasal media. By only removing half the cell media at each media change, neurons were minimally disturbed and the neurotrophic factors and other compounds released by the neuronal cultures were not completely eliminated. This is favorable to preserve neuronal cultures as the supportive environment is maintained. Neurons were cultured for 19 days post dissection before they were used for subsequent experiments.

3.4.4 Rt-PCR

Rt-PCR of mouse astrocytes and neurons was performed as previously described in section 3.3.1.1-3.3.1.3 using the following primers.

Mouse-β-actin- NM_007393.3**:** 228bp

FP 5’ CAT GGC TGG GGT GTT GAA GGT TCT

RP 5’ CGA GCC CCA GAG CAA GAG AGG T

Mouse ENT1- NM_001199116.1: 196bp

FP 5’-CAA GTA TTT CAC AAA CCG CCT GGA C

RP 5'-GAA ACG AGT TGA GGC AGG TGA AGA C

Mouse ENT2- NM_007854.3: 288bp

FP 5' GAC CTC TGC TCT TGG ATA CTT CAT

RP 5'GAC AAC AAA GAC TGA AGG TTT TCC

Mouse ENT3- NM_ 023596.3: 245bp

Mouse ENT4- NM_146257.2: 279bp

FP 5' ATT GGC GGC TGT GCT CCT AAA

RP 5' TGC CGT GCT CTC TCC AGT CAT

3.4.5 Western Blot Analysis

Mouse cortical neurons were harvested from 24 well plates, seven days after dissection, by lysing directly in Laemmli loading buffer (Sigma Aldrich; S-3401) and mouse hippocampal neurons were harvested 19 days after dissection by lysing directing in SDS-loading buffer (1 M Tris-Cl, pH 6.8, glycerol, 1% SDS, 0.5% BromoPhenol Blue, mercaptoethanol). Mouse astrocytes were grown in T-75 flask until 80% confluent at which point cell media was removed and cells were washed in PBS. Fresh NP-40 buffer was added to cell flask and cells were harvested; protein concentration was measured prior to using samples. Mouse microglial and bEND3 cells were grown in T-75 flasks and harvested by lysing cells directly in Laemmli buffer (Sigma Aldrich; S-3401).

Western Blot analysis was performed as previously described in Section 3.2.3; ENT3(N-20) diluted to 1:200 was used as the primary antibody and the corresponding secondary antibody, donkey anti-goat, was diluted to 1:5,000.

To verify consistency in amount of total protein loaded, membranes were stripped by incubating membranes in Re-Blot Plus Strong Solution (Chemicon International; CA92590) for 15 mins at RT with constant shaking. The strip solution was removed and

the membrane was incubated twice in fresh blocking buffer for 5 mins each at RT with constant shaking. Blocking buffer was removed and membranes were incubated in the control antibody, actin (Sigma-Aldrich; A5441) diluted to 1:1,000 for 1h at RT with constant shaking. The membranes were then treated as a typical western blot; membranes were washed, three times in TBS-T buffer for 10 mins each at RT with constant shaking and incubated in the appropriate secondary antibody, rabbit anti-mouse diluted to 1:20,000, for 1h at RT with constant shaking. The excess secondary antibody was removed by washing three times in TBS-T for 10 mins each at RT with constant shaking and the membrane was visualized as described in Section 3.2.3.

3.4.6 Immunocytochemistry (ICC)

3.4.6.1. Astrocytes

Mouse cortical astrocytes were grown on four chamber BD Falcon culture slides (BD Biosciences; 354104) until approximately 60% confluent. Cell media was removed and cells were washed with PBS for 5 mins at RT and incubated for 20 mins at RT in cold methanol as fixative. Methanol was removed and cells were washed three times, 5 mins each, with PBS at RT. Cells were incubated for 60 mins at RT in blocking buffer (3% normal goat serum, 0.1% triton X-100, 1% BSA in PBS). Blocking buffer was removed and cells were incubated overnight at 4°C in either blocking buffer containing no antibodies (negative control), ENT3(N-20) diluted to 1:50 in blocking buffer (Santa Cruz Biotechnologies; sc-48150), anti-glial fibrillary acidic protein (GFAP) raised in rabbit (Millipore; AB5804) diluted to 1:1,000 or a combination of the two antibodies. The following day cells were

washed five times, for 5 mins each wash, with PBS at RT. Cells were incubated with the corresponding secondary antibodies; donkey anti-goat IgG-FITC (Santa Cruz Biotechnology; sc-2024) diluted 1:200 and goat anti-rabbit IgG (H+L) 594 conjugated (Thermoscientific; 35560) diluted 1:500. Cells were incubated for 2h at RT keeping cells concealed from the light to protect the secondary antibodies. Cells were washed twice with PBS for 5 mins at RT and then twice with double distilled water for 5 mins at RT. Chamber walls of culture slides were removed and cells were allowed to air dry before mounting coverslides with Vectashield mounting medium H-1000 containing DAPI (Vector Laboratories; CA94010).

Cells were visualized using an Olympus IX51 microscope and images were captured using ImagePro Express 6.3.

3.4.6.2. Neurons

After 19 days in culture, immunostaining was performed on mouse hippocampal neurons grown on 35 mm glass bottom culture dishes (MatTek Corporation; P35G-1.5-14-C) following the protocol as previously described in Section 3.4.6.1.

Neurons were incubated overnight at 4°C in blocking buffer alone containing no antibodies, Santa Cruz ENT3(N-20) diluted to 1:50, anti-neuronal nuclei, NeuN (Chemicon International; MAB377), diluted to 1:50 or 1:100 or a combination of the two antibodies. The corresponding secondary antibodies were Donkey Antigoat IgG-FITC (Santa Cruz Biotechnology; sc-2024) diluted 1:200 and Goat Antimouse (H+L) 594 (Thermoscientific; 35501) diluted 1:500.

3.5 Mouse Brain Tissue

3.5.1 Dissections

Dissections of CD1 mice were performed graciously by Dali Zhang. Brain regions of interest, cortex, cerebellum, striatum and hippocampus, were harvested and stored immediately at -80°C until needed. Tissue was homogenized on ice, using a sonic dismembrator system 117V, 50/60Hz (Fisher Scientific), in fresh NP-40 buffer and samples were centrifuged at 12,600 rpm (14,800 x g) for 5 mins at 4°C. The supernatant was collected and the pellet (P1) was resuspended in the same lysis buffer. Protein concentration of both the supernatant and the resuspended pellet was measured as described in section 3.6.2. using diluted NP-40 buffer to prepare protein standard.

3.5.2 Rt-PCR

RNA from tissue samples was isolated using TRIzol, as previously described in section 3.3.1.1. Rt-PCR was performed immediately as described in section 3.3.1.2 and 3.3.1.3, using the slow-down program. PCR reactions were conducted using primers targeting a 228bp sequence of mouse β-actin as a positive control and a 245bp sequence of mouse ENT3. The corresponding sequences for the primers are found below. Unused sample cDNA was stored at -80°C.

Mouse-β-actin- NM_007393.3**:** 228bp
Mouse-ENT3- NM_023596.3**:** 245bp

3.5.3 Western Blot Analysis

Mouse tissue protein was prepared as previously described in section 3.5.1 and 80 µg of sample protein was separated by electrophoresis and western blot analysis was performed as previously described in section 3.2.3.

3.5.4 Differential Centrifugation

Cortex and cerebellum from CD1 mice were homogenized on ice in subcellular fractionation buffer (250 mM sucrose, 20 mM HEPES pH 7.4, 10 mM KCl, 1.5 mM $MgCl_2$, 1 mM EDTA and 1 mM EGTA) containing 1 mM DTT and a cOmplete protease inhibitor cocktail tablet. Using a sonic dismembrator system, samples were homogenized on ice and passed 10 times through a 25G needle with a 1mL syringe.

Total cell lysate was incubated for 20 mins on ice and spun at 3,000 rpm (720 x g) for 5 mins at 4°C producing P1, a pellet expected to contain the nuclear fragments, and the supernatant, which was transferred to a new Eppendorf tube. P1 was washed once by re-suspending the pellet in the subcellular fractionation buffer using a 25G needle and then centrifuged again at 3,000 rpm for 10 mins at 4°C. The wash supernatant was removed completely and P1 was resuspended in Laemmli buffer containing 10% glycerol and 0.1% SDS. The collected supernatant was centrifuged at 8,000 rpm (10,000 x g) for 5 mins at 4°C producing P2, a pellet expected to contain mitochondria, and the supernatant, which was transferred to a new tube. P2 was washed in the same manner as P1, at a speed of 8,000 rpm for 10 mins at 4°C and then resuspended in the above Laemmli buffer. The collected

supernatant from the second spin was centrifuged using a Sorval WV Ultra 90 Series centrifuge, T-1250 rotor (Thermo Electron Corporation) at 40,000 rpm (100,000 x g) for 60 mins at 4°C. A third pellet, P3, expected to contain plasma membranes was collected. The final supernatant containing cytosolic proteins was transferred to a new tube; as the final supernatant was already suspended in fractionation buffer, sample was added directly to Laemmli loading buffer at a 1:1 ratio. P3 was washed identically to P1, centrifuged at a speed of 40,000 rpm for 45 mins at 4°C and then resuspended in the above Laemmli.

3.6 Functional Studies of mENT3

3.6.1 Release Assay

WT and transfected HEK 293T cells were plated on 12 well plates at a density to allow 80-90% confluency on the day of assay.

All buffers were prepared fresh on the day of the assay. Two buffers were prepared, one contained 11 mM glucose (Acros Organics) (+) and one with glucose replaced with 10 mM 2-deoxyglucose (2-DG) (-); both buffers contained a final concentration of 25 mM HEPES, 4.9 mM KCl, 1.2 mM $MgCl_2$, 1.4 mM KH_2PO_4 (Fisher Scientific), 1 mM $CaCl_2$ (Mallinckrodt), 118 mM NaCl. Buffers were made to a final pH of 7.4 (Accumet Basic AB15 pH Meter; Fisher Scientific) and an osmolarity of 300+/-10 mOsm as determined by VAPRO Vapor Pressure Osmometer 5520 (Vescor). [^{3}H]adenine solution (250 MBq) (PerkinElmer; NET053) was made in buffer (+) whereas 10 mM 2-DG and a third solution

containing 10 mM 2-DG and 30 µM DPR (Sigma-Aldrich) were prepared in buffer (-). All buffers and solutions were prewarmed to 37°C.

To tritiate cellular ATP, cell media was removed and cells were washed twice with physiological buffer containing glucose then incubated with [^{3}H]adenine solution for 30 mins at 37°C. To remove extracellular [^{3}H]adenine,the solution was removed and cells were washed twice with physiological buffer without glucose. Cells received one of three possible treatments (0.5 mL per well) and were incubated for 30 mins at 37°C; physiological buffer containing glucose, subjected to glucose deprivation using 2-DG solution or a combination of glucose deprivation, 2-DG, in presence of DPR. The supernatant was collected from each treatment group following incubation and 0.35 mL of the supernatant was used to determine extracellular radioactivity by scintillation spectroscopy using Beckman Coulter LS 6000TA. Cells were dissolved overnight in 0.5 mL of 1M NaOH at 37°C; 0.35 mL used to determine intracellular radioactivity and the remainder was used to measure protein content of each well. To neutralize the NaOH of the intracellular components, 28 µL of HCl was added prior to counting samples; 28 µL of HCl was previously determined as sufficient to bring the samples to neutral pH.

3.6.2 Protein Assay

Using a 96 well plate the protein content of each well was determined with the collected intracellular contents compared to a protein standard using BSA (Sigma; A-7906) in 1 M NaOH buffer diluted to 1:20. Preparation of the standard had an initial well concentration of 0.5 mg/mL, by mixing 160 µL of diluted NaOH (1:20) and 160 µL of BSA protein (1

mg/mL), and a final well concentration of 0.00781 mg/mL. A blank, containing only diluted NaOH was also prepared. Intracellular samples were diluted to 1:20 in double distilled water and protein content was measured in duplicate. 40 µL of BioRad dye was added to each well and mixed completely. Plates were read using SynergyHT (Biotek Instruments, Inc.) a wavelength of 595 nm. Optical density values of samples were converted to mg/ml using the BSA standard curve using Gen5 software v.1.01.14.

3.6.3 Quantification of Purines

Thin-layer chromatography (TLC), as described by Schrader and Gerlach (1976), was performed to identify purines released from WT and transfected HEK293T cells during the release assay described in section 2.6.1. Extracellular supernantants (20 µL) were combined with a cold carrier (5 µL) containing AMP, inosine, xanthine, hypoxanthine and adenosine, each at 15 mM, and spotted on Uniplate gel-silica plates (Fisher Scientific; 05719803). Solvent containing n-butanol, ethyl acetate, methanol and ammonium hydroxide (7: 4: 3: 4) was used for purine separation. From the bottom of the plate, purines separated in the following order: AMP, INO, Xa, HX and ADO and spots were visualized under UV light and marked. Spots of interest were removed from the plates and dissolved in 500 µL 0.2M HCl for 20 mins before adding scintillation fluid to the samples. Radioactivity was determined by scintillation spectroscopy. Purines were quantified using the specific activity of the [^{3}H]adenine loading solution.

Chapter 4

Results

4.1 The pIRES-puro-Flag-mENT3 Plasmid

Commercial antibodies are valuable tools that can be used to visualize, quantify and isolate specific endogenous proteins. However, antibodies for the subtypes of ENTs have been problematic as many commercial antibodies are of low affinity and low specificity. For this reason, experiments were performed to confirm that the commercial antibody for ENT3 was of high specificity.

An important control for the use of an antibody is to show that the antibody recognizes a protein of the expected molecular weight in cells or tissues known to express the protein and not in cells or tissues that do not express the protein. A common strategy is to transfect cultured cells with an expression plasmid that contains the coding sequence for the target protein, in this case a pIRES-puro-Flag-mENT3 plasmid.

Prior to testing the commercial ENT3 antibody, the mENT3 gene insert had to be designed and correctly ligated within the plasmid. Cultured astrocytes, tested by RT-PCR, were found to express the mouse ENT3 gene; cDNA template was probed with a primer pair targeting the mouse GAPDH gene, as a template control, or a primer pair targeting the

mouse ENT3 gene sequence (Figure 1). Presence of a band at the expected size indicates mouse astrocyte cDNA as an acceptable source for the mouse ENT3 gene sequence.

To ensure sufficient mENT3 DNA for plasmid insert design, multiple PCR reactions were performed using mouse cortical astrocyte cDNA as the template source (Figure 2). The primers were modified to include the restriction sites corresponding to Asc1 and Not1; to facilitate ligation with the plasmid, pIRES-puro-Flag. Bands of the expected size were excised from the gel and harvested cDNA was purified.

Collected PCR product was subjected to restriction digestion to create sticky ends. Restriction digestion of the pIRES-puro-Flag plasmid was also performed and then ligation of the PCR product and the plasmid was completed. *E. coli* was transformed with the resulting recombinant plasmid and grown on LB plates containing ampicillin overnight. Twelve individual transformants were selected from the LB plates and plasmid DNA was isolated and subjected to diagnostic restriction digestion using Nhe1 (Figure 3). Of these 12, two were found to have the expected fragment sizes; the corresponding transformant of #11 was further cultured in LB broth to increase the amount of total plasmid yield. Purified plasmid DNA was sequenced by MICB to determine the precise insert sequence (Figure 4) and the corresponding amino acid sequence (Figure 5). All changes in gene insert sequence are identified in italics/boxes and were found to be declared SNPs on NCBI.

The complete pIRES-puro-Flag-mENT3 plasmid contains a CMV-promoter, two coding genes conferring resistance to ampicillin and puromycin, the mENT3 gene insert and a flag-tag found at the N-terminus of the insert (Figure 6).

Following confirmation of the pIRES-puro-Flag-mENT3 gene sequence, HEK293T were transfected using jetPRIME transfection reagent. A stable transfected cell line was established using puromycin antibiotic due to plasmid-mediated resistance conferred with successful incorporation of the pIRES-puro-Flag plasmid. WT and transfected cells were harvested and western blot analysis was performed comparing identical samples probed with an antibody targeting the Flag epitope, Anti-Flag M2 Peroxidase, or with a commercial antibody targeting the ENT3 protein (Figure 7). Although not of the expected size, reported by the manufacturer to be 52kD, both the Anti-Flag M2 and the ENT3 antibody showed identical band sizes in the transfected cell line. Based on the consistency of band sizes, it was concluded that the commercial ENT3 antibody was specific to the ENT3 protein.

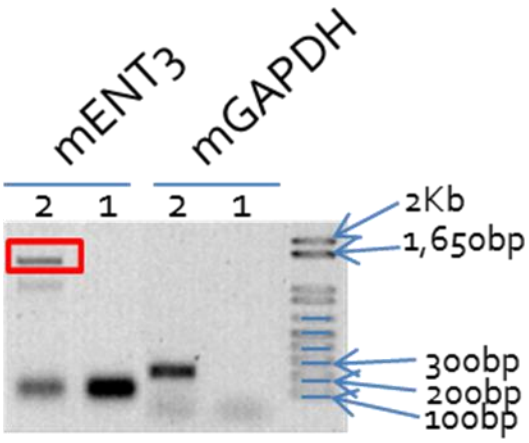

Figure 1 Verification of ENT3 expression in Mouse Cortical Astrocytes by RT-PCR

Total RNA isolated from cultured mouse cortical astrocytes was reverse transcribed then used in a PCR reaction to confirm the expression of the ENT3 gene. cDNA template was probed with a mouse GAPDH primer pair, designed to amplify a sequence of 228bp, or with a mouse ENT3 primer pair designed to amplify the entire open reading frame of 1.4Kb. PCR products were subjected to electrophoresis and bands were visualized under UV light.

Lane 1 no template control; lane 2 mouse cortical astrocyte cDNA.

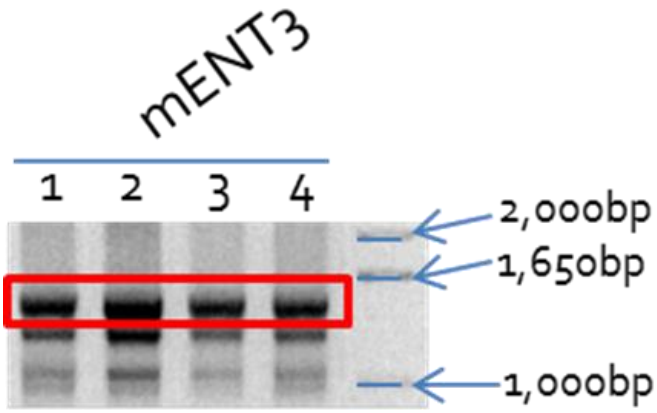

Figure 2 Collection of Mouse ENT3 cDNA from Mouse Cortical Astrocytes by PCR

Total RNA samples from cultured mouse cortical astrocytes were subjected to RT-PCR. Using modified mENT3 primer pairs containing AscI and Not1 restriction sites, astrocyte cDNA template was assessed for mENT3 expression. Modified primer pairs target a gene sequence of 1.4Kb. Electrophoresis was performed with PCR products and bands were visualized under UV light. The bands of the expected size were excised from the agarose gel and collected.

Red box indicates bands of interest (1.4Kb).

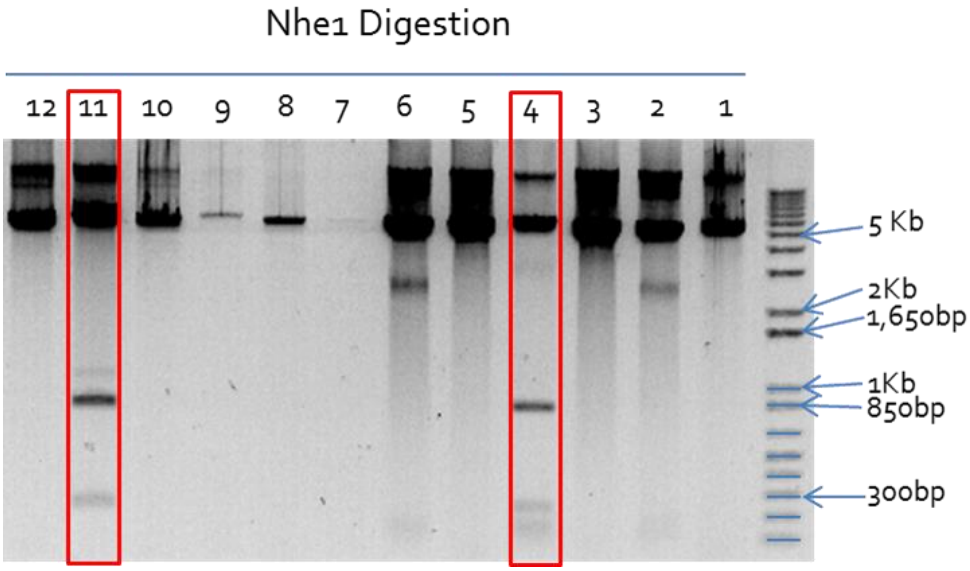

Figure 3 Verification of Plasmid Inserts Collected from Transformed E. coli Starter Cultures

Transformed E. coli cultures were grown overnight and plasmid DNA was collected the following day. Samples were digested using Nhe1 restriction enzyme as an initial diagnostic of plasmid insert, pIRES-puro-Flag-mENT3. Following digestion, electrophoresis was performed with all samples whereby successful ligation was expected to present three fragments of the following sizes: 226bp, 771bp and 5.6Kb. Restriction enzyme digestion was intended as an initial means of plasmid insert verification; the insert sequence was confirmed by the Manitoba Institute of Cell Biology.

Lanes 1-12 contain plasmid DNA isolated from twelve individual starter colonies.

Red boxes indicate samples with the correct band sizes indicative of successful ligation. The culture corresponding to lane 11 was used for all further experiments.

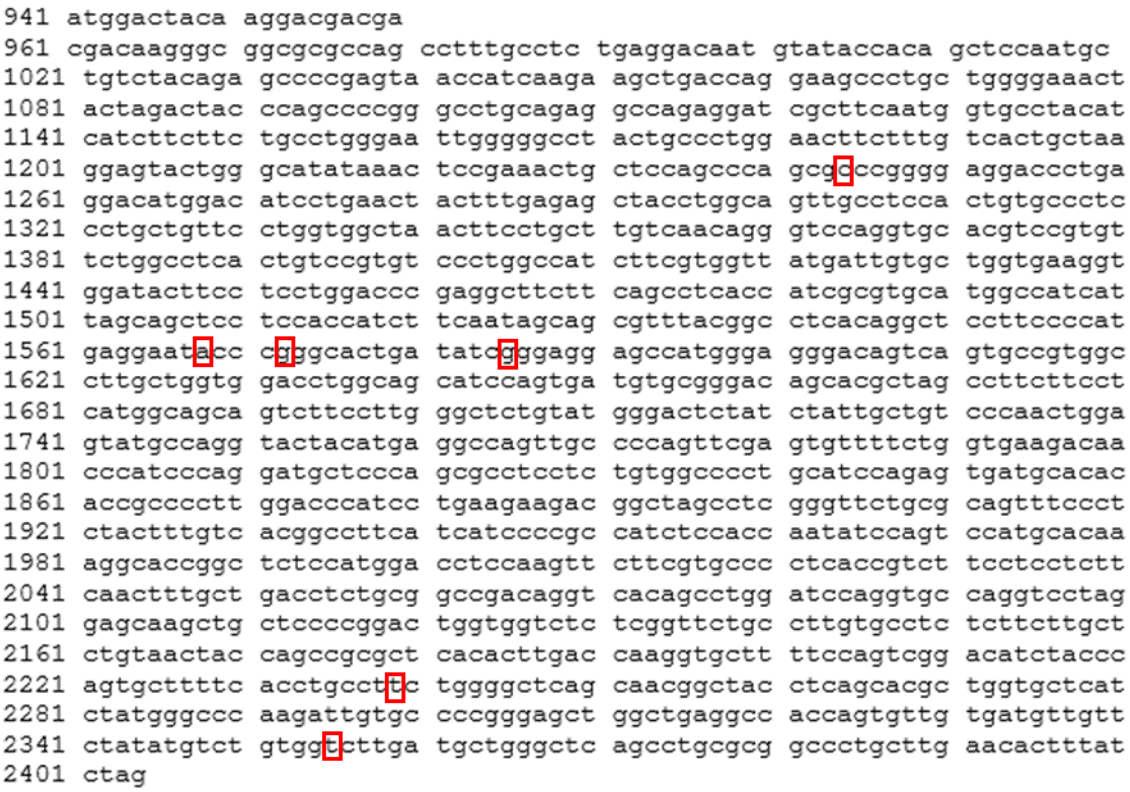

Figure 4 Sequencing Results for pIRES-puro-Flag-mENT3 plasmid DNA

Plasmid DNA was collected from transformed E.coli cultures and subjected to diagnostic restriction digestion with Nhe1. The E. coli culture corresponding to a successful digestion was further grown to increase plasmid yield. Purified plasmid DNA was combined with primers designed for mENT3 gene sequencing, identified as CMV-F, mENT3-419-F and mENT3-911-F. Samples were sent for sequencing at MICB. Complete sequencing allows for identification of any errors within the insert sequence including insertions, deletions and mismatches.

Red boxes indicate single-base variations (SNPs) from the Genbank sequence: 1244T→C, 1568G→A, 1572A→G, 1585A→G, 2239C→T and 2355G→T.

MDYKDDDDKG GAPAFASEDN VYHSSNAVYR APSNHQEADQ EALLGKLLDY PAPGLQRPED
RFNGAYIIFF CLGIGGLLPW NFFVTAKEYW AYKLRNCSSP APGEDPEDMD ILNYFESYLA
VASTVPSLLF LVANFLLVNR VQVHVRVLAS LSVSLAIFVV MIVLVKVDTS SWTRGFFSLT
IACMAIISSS STIFNSSVYG LTGSFPMRNT RALISGGAMG GTVSAVALLV DLAASSDVRD
STLAFFLMAA VFLGLCMGLY LLLSQLEYAR YYMRPVAPVR VFSGEDNPSQ DAPSASSVAP
ASRVMHTPPL GPILKKTASL GFCAVSLYFV TAFIIPAIST NIQSMHKGTG SPWTSKFFVP
LTVFLLFNFA DLCGRQVTAW IQVPGPRSKL LPGLVVSRFC LVPLFLLCNY QPRSHLTKVL
FQSDIYPVLF TCLLGLSNGY LSTLVLIYGP KIVPRELAEA TSVVMLFYMS VVLMLGSACA
ALLEHFI

Figure 5 Translated Amino Sequence for pIRES-puro-Flag-mENT3 plasmid DNA

Plasmid DNA was harvested and then purified from transformed E. coli cultures that had initially been tested by diagnostic restriction digestion using Nhe1. Plasmid DNA was combined with primers CMV-F, mENT3-419F and mENT3-911F and sequenced at MICB.

Blue box indicates initiator; red box indicates flag-tag epitope.

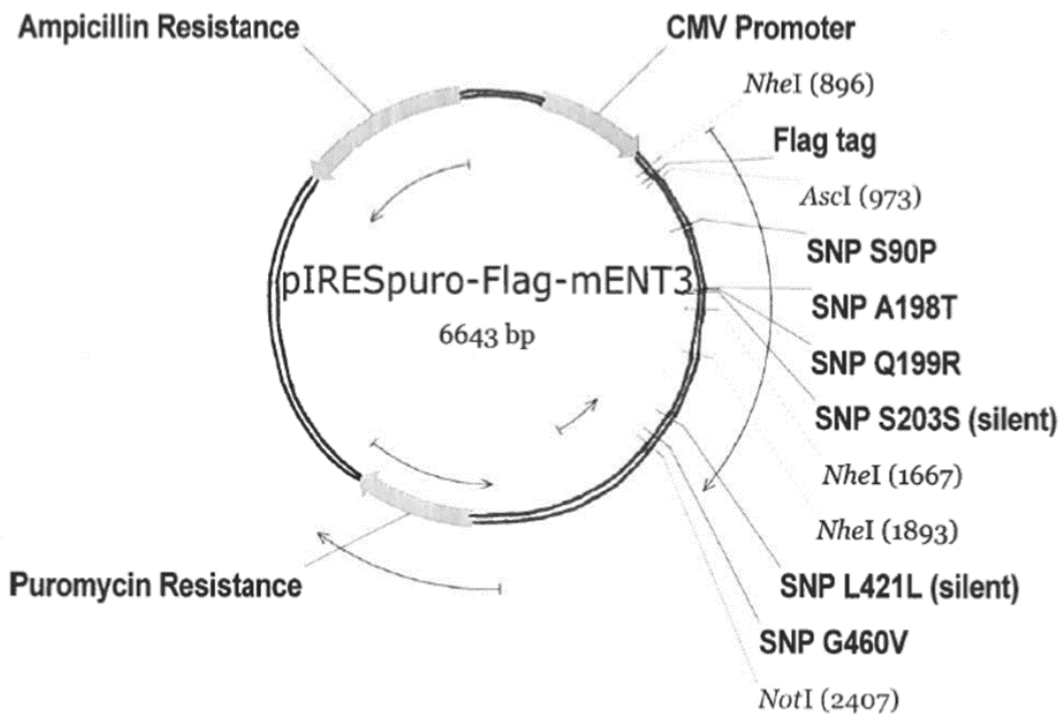

Figure 6 Plasmid Map of pIRES-puro-Flag-mENT3

Mouse ENT3 gene sequence was inserted into the pIRES-puro-Flag plasmid; plasmid insert sequence was confirmed by the MICB. Key sites within the plasmid sequence have been indicated on the plasmid map. The location of the CMV promoter and Flag-tag can be found at the N terminus of the mENT3 insert. Six SNPs within the insert sequence were identified and are labeled on the plasmid map. Digestion sites of Not1 and Asc1, the restriction enzymes used to perform ligation by which the mENT3 gene was incorporated into the pIRES-puro-Flag plasmid, are indicated. In addition, the digestion sites of Nhe1, the RE used as an initial means of confirming plasmid insert, have been labeled. The position of all RE digestion sites has been included in parenthesis next to each RE.

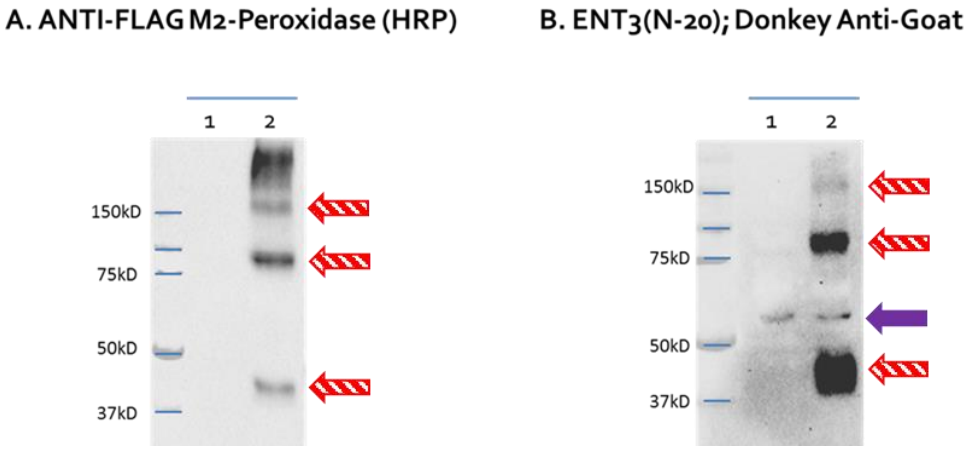

Figure 7 Western Blot Analysis to Confirm Specificity of Commercial ENT3 Antibody

HEK293T cells were transfected using jetPRIME transfection reagent and stable transfected cells were established by puromycin selection. WT and transfected HEK293T cells were harvested and western blot analysis was performed using 40µg of cell protein. Identical samples were probed with (A) Anti-Flag M2-Peroxidase (HRP), an antibody specific for the Flag epitope, diluted to 1:1,000 and (B) with a commercial antibody targeting ENT3(N-20) diluted to 1:200 with the corresponding secondary antibody, donkey anti-goat diluted to 1:5,000.

Lane 1 WT HEK293T cells; lane 2 transfected HEK293T cells

Red arrows indicate identical sized bands (ENT3); purple arrow indicates endogenous protein (hENT3).

4.2 Characterization of HEK293T Cells

As HEK293T cells had not previously been characterized for endogenous ENT family expression (ENT1-4), RNA was isolated from WT as well as from transfected cells and reverse transcription was performed. PCR was completed using primer pairs targeting the human subtypes of ENT (ENT1-4), in addition to a primer pair targeting the mouse ENT3 gene. Electrophoresis was performed with all PCR products whereby a band of the expected size, specific to each primer pair, indicated endogenous mRNA expression in HEK293T cells (Figure 8). cDNA of WT and transfected cells was probed with the mouse ENT3 primer pair for two reasons, as an initial means of verifying success of transfection and to investigate the possibility of cross-reactivity between human and mouse ENT3 sequences.

qPCR was performed comparing WT and transfected HEK293T cells. Although Rt-PCR was an initial means of determining RNA expression, qPCR offers more detailed information including relative levels of ENT subtypes and is a measure of transfection efficiency. cDNA derived from WT and transfected cells was combined with LuminoCt Ready Mix and individual reactions were made up of a primer pair targeting each of the four ENT subtypes and a primer pair targeting the mouse ENT3 gene (Figure 9). A primer pair targeting the human β-actin gene was used as a template control.

Transfection of HEK293T cells was not found to affect endogenous ENT family expression; ENT2 was discovered to be most highly expressed followed by ENT1, ENT4 and ENT3. The mENT3 primer pair showed no cross reactivity with hENT3 gene and transfection was determined to be successful.

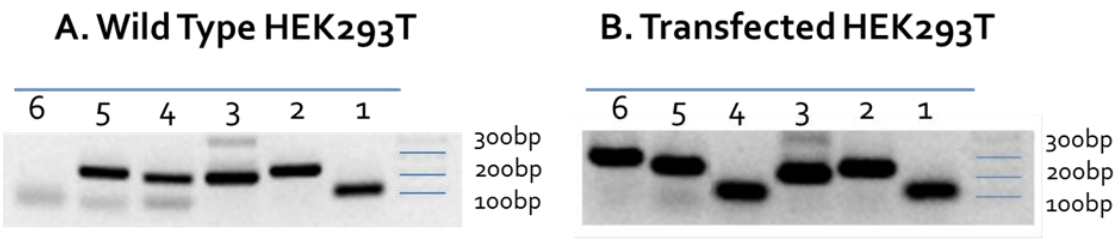

Figure 8 Characterization of WT and Transfected HEK293T Cells

cDNA of WT and transfected HEK293T cells was prepared and PCR was performed to determine endogenous expression of the four members of the ENT family (ENT1-4). cDNA was probed with a primer pair targeting the β-actin gene, designed to amplify a gene sequence of 116bp or with primer pairs targeting hENT1, amplifying a gene sequence of 227bp, hENT2 amplifying a gene sequence of 196bp, hENT3 amplifying a gene sequence of 188bp or hENT4 amplifying a gene sequence of 203bp. In addition, both WT and transfected cells were probed with a primer pair targeting the mENT3 gene, designed to amplify a band of 245bp.

Lane 1 β-actin; lane 2 hENT1; lane 3 hENT2; lane 4 hENT3; lane 5 hENT4; lane 6 mENT3

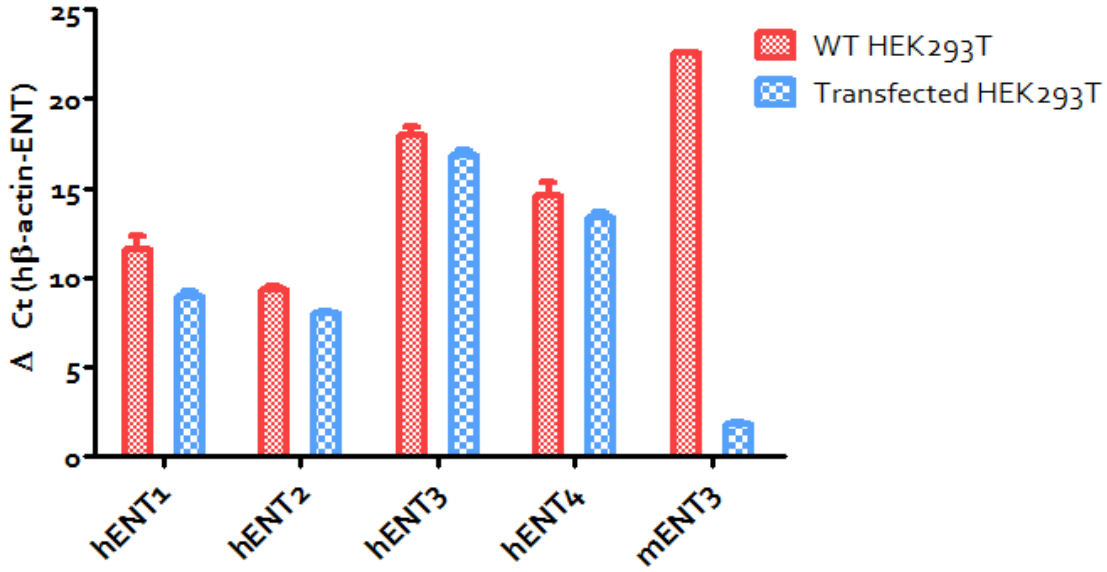

Figure 9 Comparison of Expression Levels of WT and Transfected HEK293T Cells by qPCR

HEK293T cells were transfected with pIRES-puro-Flag-mENT3 plasmid using jetPRIME reagent and stable transfected colonies were established with puromycin selection. RNA was isolated from both WT and transfected HEK293T cells and reverse transcription was performed. Using LuminoCt ReadyMix protocol, prepared cDNA template was combined with primer pairs targeting the four human ENT subtypes as well as with a primer pair targeting the mENT3 gene. Relative expression levels of WT and transfected cells were assessed by two-way ANOVA.

ΔCt was calculated based on the expression level of h-β-actin, a known housekeeping gene used as a positive control.

4.3 Assessment of ENT3 Localisation

Determination of the localisation of ENT3 could indicate possible functions of this transporter. CD1 mice were dissected and the cortex, cerebellum, striatum and hippocampus were harvested. Reverse transcriptase was performed with each brain region and prepared cDNA was used for PCR. cDNA template was probed with a primer pair targeting the mouse β-actin gene or with a primer pair targeting the mouse ENT3 gene sequence. PCR products were separated by electrophoresis and bands were visualized by UV light; positive bands confirm endogenous mRNA of ENT3 within each particular brain region (Figure 10).

As mRNA expression does not necessarily correlate with the level of protein expression, western blot was performed to assess the presence of ENT3 protein. Brain regions of interest, cortex, cerebellum, striatum and hippocampus, were harvested from CD1 mice. Protein samples were probed with the ENT3(N-20) antibody, with an expected band size of 52 kD (Figure 11A). Subsequently, membranes were stripped of initial antibodies and probed with an antibody targeting actin, as a loading control (Figure 11B). Of the four brain regions tested, all showed bands at the expected size of 52 kD, in addition to a second band at approximately 30 kD.

To further examine the localisation of ENT3, primary cell cultures of mouse cortical neurons and astrocytes were tested for endogenous mRNA and protein expression. RNA was isolated from cell cultures and reverse transcription was performed. cDNA template from mouse neurons or astrocytes was combined with primer pairs designed to target the mouse β-actin gene, as a template control, and each of the four mouse ENT subtypes

(mENT1-4). PCR products were subjected to electrophoresis and bands were visualized under UV light (Figure 12). Presence of a band at the expected size, as determined by the primer pair, indicates endogenous mRNA expression of the four ENT subtypes within neurons (Figure 12.A) and within astrocytes (Figure 12.B).

Western blot analysis was completed to examine ENT3 protein expression within mouse cortical neurons, mouse cortical astrocytes, mouse cortical microglia and bEND3 cells. Total astrocyte protein was harvested in lysis buffer and protein concentration was measured, all other samples were harvested directly in loading buffer to maximize protein concentrations. Western blot analysis was performed and samples were probed with the ENT3(N-20) antibody targeting ENT3 (Figure 13.A). Subsequently, membranes were stripped and samples were reprobed with an antibody targeting actin to determine total protein loaded (Figure 13.B).

Based on the expected size of 52 kD, both hippocampal neurons and astrocytes were found to express ENT3, although astrocytes showed a second band at 30 kD. Microglia and bEND3 cells were negative for ENT3 protein expression (Figure 13A). In contrast to hippocampal neurons, cortical neurons showed a much larger than expected band size, of approximately 125 kD which could indicate ENT3 protein interactions or aggregates.

Following positive western blot results, immunocytochemistry of cultured cortical astrocytes was performed. Astrocytes were costained with the ENT3(N-20) antibody specific for ENT3 and an antibody targeting GFAP, a known astrocyte marker (Figure 14).

Fluorescent images indicated ENT3 was expressed within astrocytes, primarily located within the cytosol surrounding the nucleus, and was not found to be directly colocalised

with GFAP. There was no staining when the primary antibodies were omitted, indicating that there was very little nonspecific binding of secondary antibodies.

Immunocytochemistry was also performed with hippocampal neurons based on positive results with western blot (Figure 13). Cells were costained with DAPI, a nuclear marker, an antibody targeting NeuN, a known neuronal marker found within the cytosol of neurons and the ENT3(N-20) antibody specific for ENT3 (Figure 15). A no primary control was performed to verify specificity of secondary antibodies.

The no primary control images showed high background of FITC Donkey anti-goat, but background was found to be nonspecific. Comparison of both secondary antibodies indicates distinct wavelengths as images were not superimposable confirming staining with primary antibodies. Fluorescent images of neurons indicate intracellular localisation of ENT3, primarily located surrounding the nucleus although staining throughout the cytosol and along dendrites is also visible.

To further characterize the subcellular localisation of ENT3 *in vivo*, cortex and cerebellum from CD1 mice were harvested and subjected to subcellular fractionation. This enabled separation of the brain tissue samples into four distinct fractions: nuclear, mitochondrial, membrane and cytosolic. Western blot analysis was performed with the isolated subcellular fractions and protein samples were probed with the ENT3(N-20) antibody, with an expected band size of 52 kD (Figure 16).

The final fraction, containing the cytosolic components, was positive for a band of 52 kD whereas the nuclear, mitochondrial and plasma membrane fractions showed a single, smaller band of 30 kD. This procedure was repeated with identical results.

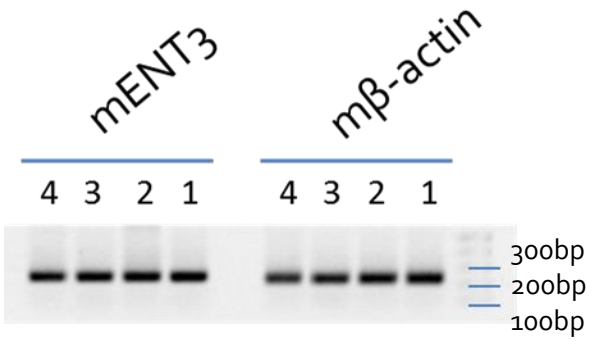

Figure 10 Endogenous Expression of ENT3 in Isolated Brain Regions

CD57 mice were dissected and cortex, cerebellum, hippocampus and striatum were harvested. cDNA was prepared from tissue samples and probed with a primer pair targeting mouse β-actin, as a positive control, designed to amplify a sequence of 228bp or a primer targeting the mouse ENT3 gene, designed to amplify a sequence of 245bp. PCR products were run on an agarose gel and bands were visualized under UV light exposure.

Lane 1 mouse cortex; lane 2 mouse cerebellum; lane 3 mouse striatum; lane 4 hippocampus.

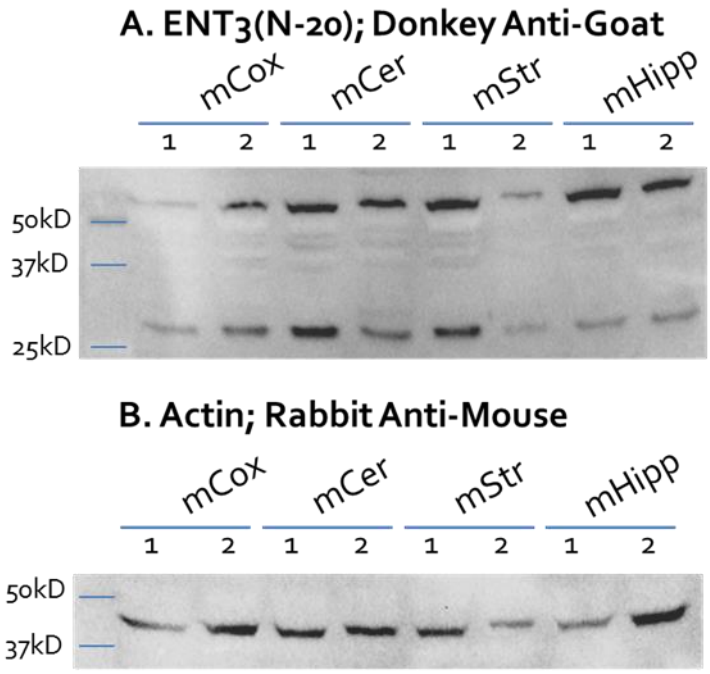

Figure 11 Verification of ENT3 Protein Expression in Brain Regions by Western Blot Analysis

CD57 mice were dissected and cortex, cerebellum, hippocampus and striatum were harvested. Samples were homogenized and centrifuged at 12,600 rpm for 5 mins at 4°C. Western blot analysis was performed using both the supernatant and the resuspended pellet; 80 µg of protein for each sample was loaded excluding mouse striatum which only contained 45µg. The membrane was incubated with the ENT3(N-20) antibody (A) with an expected band size of 52 kD, diluted to 1:200, with the appropriate secondary antibody, donkey anti-goat diluted to 1:5,000. Bands were visualized before the membrane was stripped and reprobed for actin, as a loading control (B), diluted to 1:1,000, with the appropriate secondary antibody, rabbit anti-mouse diluted to 1:10,000.

Lane 1 supernatant; lane 2 resuspended P_1.

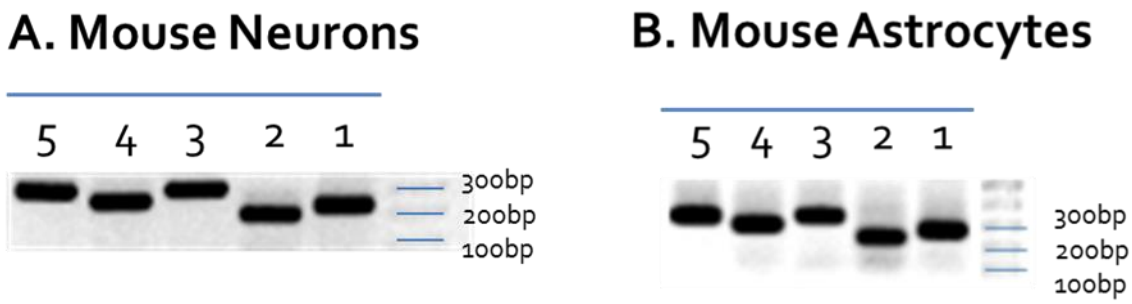

Figure 12 Characterization of Primary Mouse Neurons and Astrocytes

RNA from mouse cortical neurons and astrocytes was isolated and reverse transcription was performed. PCR was completed using cDNA templates combined with primer pairs targeting the four subtypes of ENT family; mENT1 designed to amplify a gene sequence of 196bp, mENT2 designed to amplify a gene sequence of 288bp, mENT3 designed to amplify a gene sequence of 245bp and mENT4 designed to amplify a gene sequence of 279bp. In addition, cDNA templates were tested with a primer pair targeting the mouse β-actin gene, designed to amplify a gene sequence of 188bp, as a positive control. Electrophoresis was performed with PCR products and bands were visualized under UV light.

Lane 1 β-Actin (228bp); lane 2 mENT1 (196bp); lane 3 mENT2 (288bp); lane 4 mENT3 (245bp); lane 5 mENT4 (279bp).

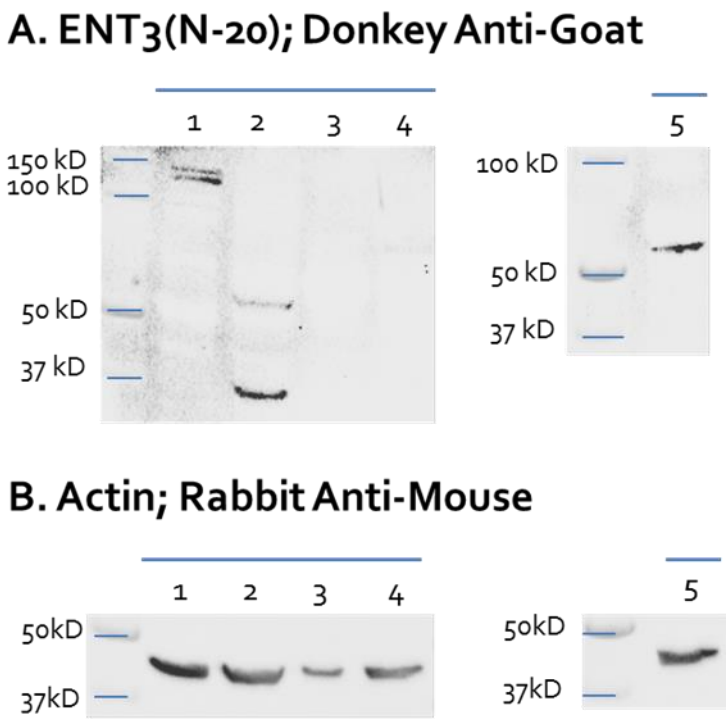

Figure 13 ENT3 Found to be expressed in Mouse Neurons and Astrocytes but not in Microglial or bEND3 cells

Protein was harvested from mouse cortical and hippocampal neurons, mouse cortical astrocytes, mouse cortical microglia and bEND3 cells and samples were subjected to western blot analysis to assess ENT3 protein expression. Protein concentration of mouse astrocytes was determined and 80µg was loaded. Protein samples were probed with a commercial ENT3(N-20) antibody, diluted to 1:200, and bands were visualized (A). As indicated by the manufacturer, the expected band size of ENT3 was 52 kD. Repeated western blots show neurons to have one clean band at about 52 kD and astrocytes to have a primary band at about 30kD but further secondary banding is also seen. Microglia and bEND3 cells show no bands. Membranes were stripped and reprobed with an antibody targeting actin as a loading control (B).

Lane 1 mouse cortical neurons; lane 2 mouse cortical astrocytes; lane 3 mouse cortical microglia; lane 4 bEND3 total cell lysate; lane 5 mouse hippocampal neurons.

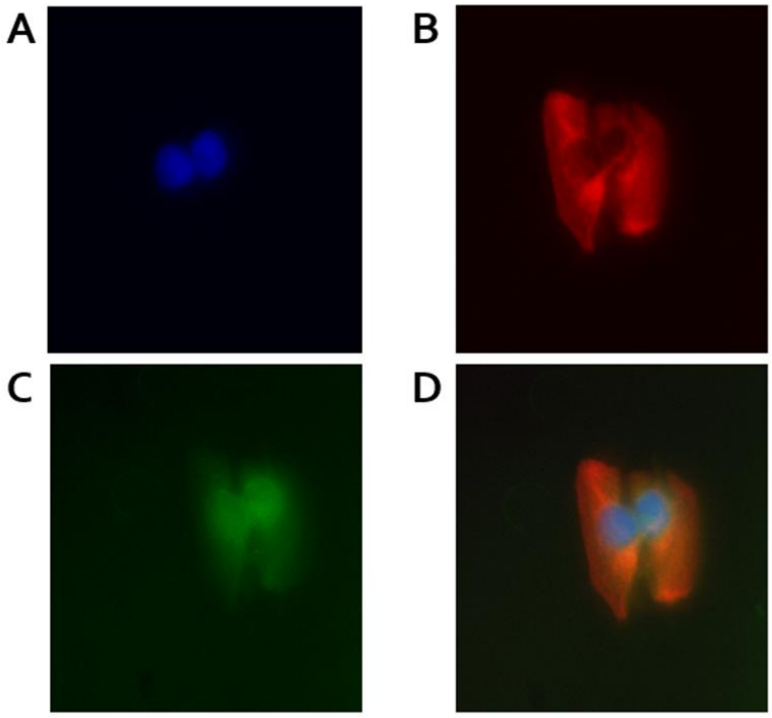

Figure 14 Immuncytochemistry of Mouse Cortical Astrocytes Indicates Localisation of ENT3 within Astrocytes in Proximinity to the Nucleus

Cortical astrocytes were harvested from CD1 mice and grown on four chamber culture slides until 60% confluent. Astrocytes were incubated overnight with an antibody specific for ENT3 (1:50), an antiGFAP antibody (1:200) or costained with both ENT3 and GFAP antibodies simultaneously. Cultures were incubated in the corresponding fluorescent secondary antibodies. In addition, a no primary control was performed in which cultured astrocytes were incubated in buffer alone, containing no primary antibodies, and subsequently incubated in both secondary antibodies. This allowed assessment of secondary antibody specificity.

FITC Donkey antigoat (1:200) corresponded to the ENT3 antibody and AlexaFluor 594 Donkey antirabbit (1:500) corresponded to GFAP antibody.

Vectashield mounting medium containing DAPI was used to mount cover slides and enabled visualization of the nucleus.

A- Dapi; B- GFAP; C-ENT3; D- Composite image

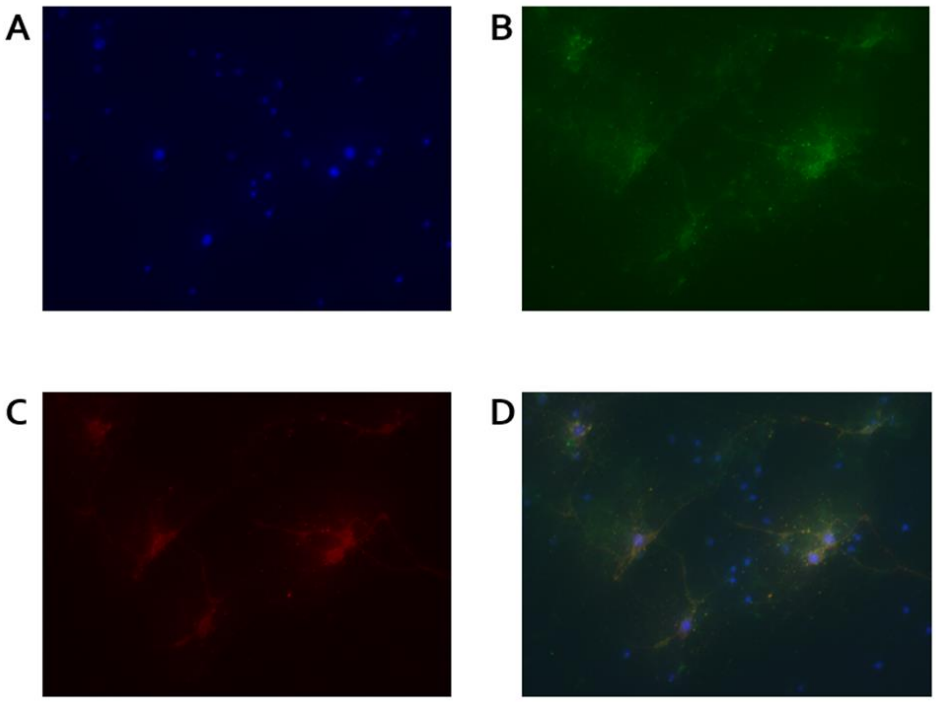

Figure 15 Immuncytochemistry of Mouse Hippocampal Neurons Indicates Intracellular Localisation of ENT3

Hippocampal neurons were harvested from CD1 mice and grown on 35 mm glass bottom culture dishes for 19 days after dissection. Neurons were incubated overnight with an antibody specific for ENT3 (1:50), an antiNeuN antibody (1:25) or costained with both ENT3 and GFAP antibodies simultaneously. Cultures were incubated in the corresponding fluorescent secondary antibodies. In addition, a no primary control was performed in which cultured astrocytes were incubated in buffer alone, containing no primary antibodies, and subsequently incubated in both secondary antibodies. This allowed assessment of secondary antibody specificity. Cell nuclei were stained using Dapi (1:1,000) for 5 mins prior to visualizing.

FITC Donkey AntiGoat (1:200) corresponded to the ENT3 antibody and AlexaFluor 594 Donkey AntiRabbit (1:500) corresponded to NeuN antibody.

A- Dapi; B- ENT3; C- NeuN; D- Composite image

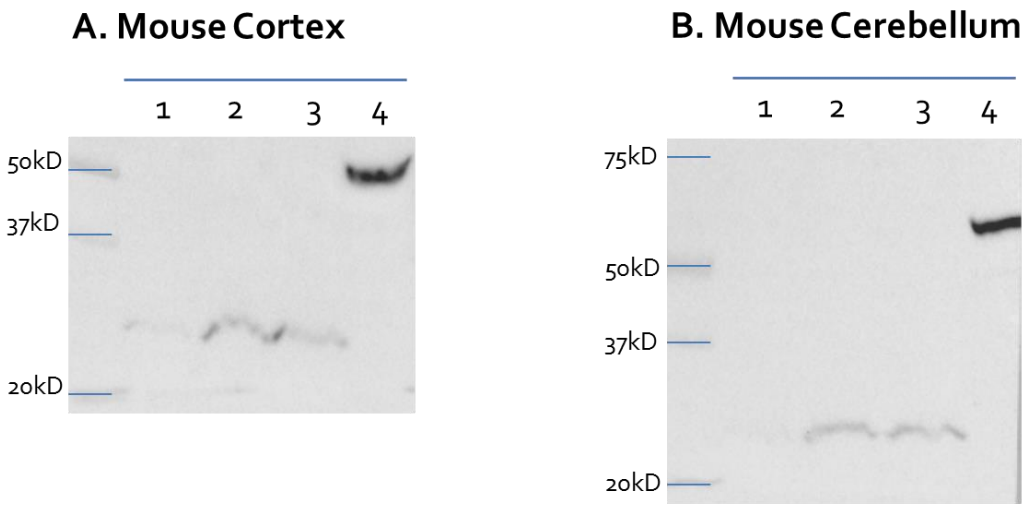

Figure 16 Differential Centrifugation of Mouse Brain Indicates Cytoplasmic Localisation of ENT3

CD1 mice were dissected and cortex and cerebellum were harvested and homogenized. Subcellular fractionation protocol was performed with both tissue samples to isolate four distinct fractions: nuclear, mitochondrial, plasma membrane and cytosolic components. Isolated fractions were subjected to western blot analysis and probed with the ENT3(N-20) antibody, with an expected band size of 52kD.

Lane 1 nuclear fraction (P_1); lane 2 mitochondrial fraction (P_2); lane 3 plasma membrane fraction (P_3); lane 4 cytosolic fraction (S)

4.4 Functional Studies of mENT3

As an initial test of ENT3 function in adenosine signalling pathways, purine release assays were performed. WT and transfected HEK293T cells were incubated with tritiated adenine to radiolabel intracellular ATP. Cells were then treated with 2-DG to induce ATP-depletion and cellular release of purine nucleosides (Figure 17). 2-DG produced a similar increase in purine release from WT and transfected HEK293T cells. DPR, an inhibitor of ENT1 and ENT2, was similarly effective at inhibiting purine release from the two cell types. Following TLC separation, it was found that inosine was the primary nucleoside released by 2-DG treatment and no cell-type difference was observed (Figure 18).

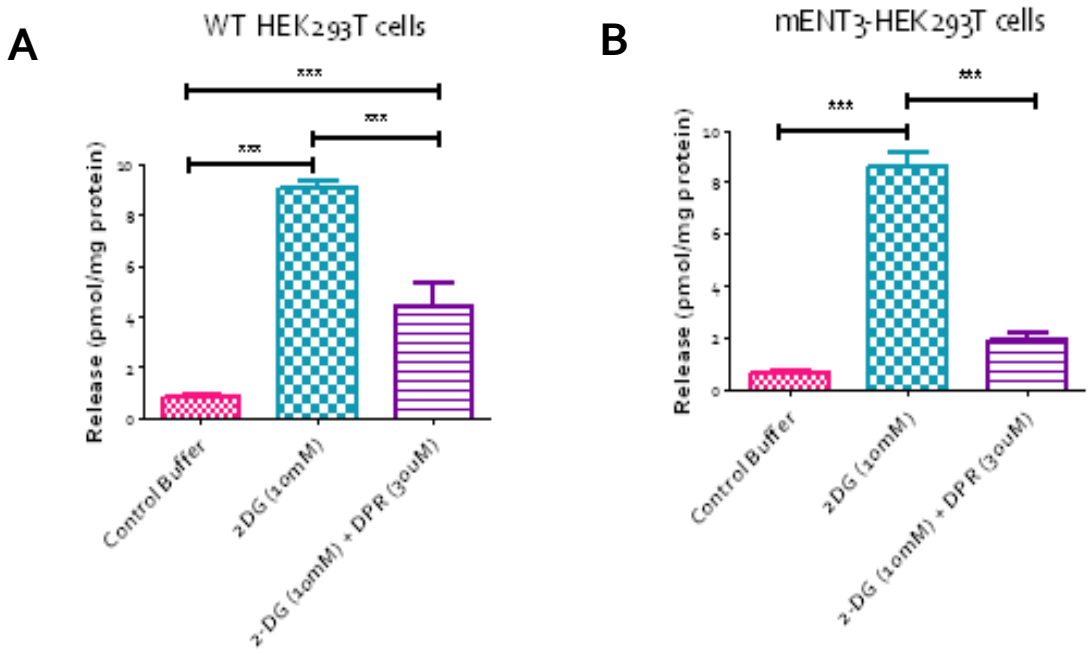

Figure 17 Transfected HEK293T cells are More Susceptible to DPR Inhibition Resulting in a Decrease in Purine Release

*WT (A) and transfected HEK293T (B) cells were grown to 80% confluence in 12 well culture plates and pretreated with - [^{3}H]adenine for 30 min at 37°C. Cells were subjected to one of three treatments: control (sodium buffer), 2-DG or 2-DG in combination with DPR. The radioactivity of samples was determined by scintillation spectrometry. Data expressed as N of 6 with experiments performed in quadruplicate. Results were assessed by one-way ANOVA with Tukey's post-test whereby *** indicates significance $p < 0.001$.*

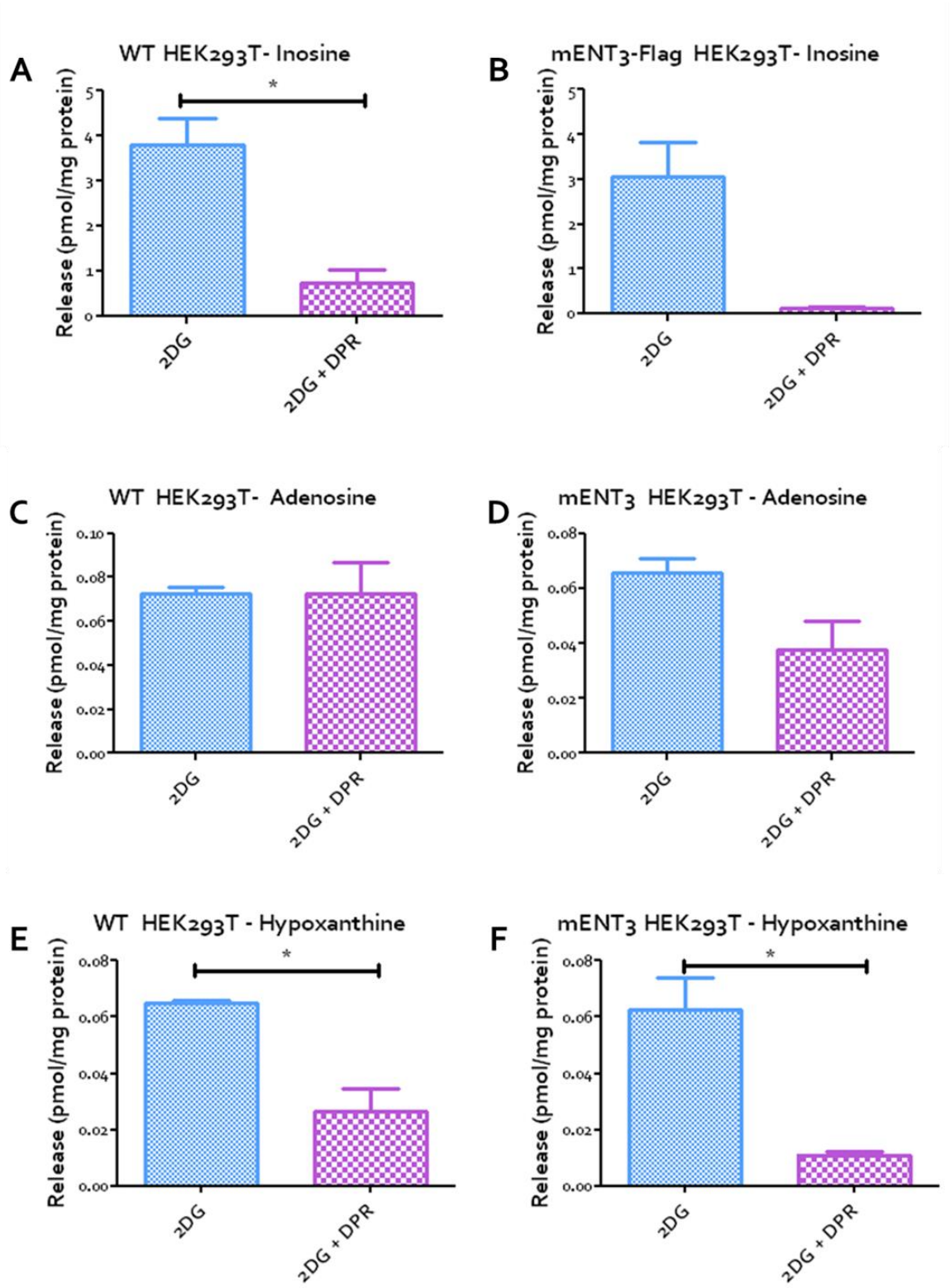
A
WT HEK293T- Inosine
Release (pmol/mg protein)
*
2DG
2DG + DPR
B
mENT3-Flag HEK293T- Inosine
Release (pmol/mg protein)
2DG
2DG + DPR
C
WT HEK293T- Adenosine
Release (pmol/mg protein)
2DG
2DG + DPR
D
mENT3 HEK293T - Adenosine
Release (pmol/mg protein)
2DG
2DG + DPR
E
WT HEK293T - Hypoxanthine
Release (pmol/mg protein)
*
2DG
2DG + DPR
F
mENT3 HEK293T - Hypoxanthine
Release (pmol/mg protein)
*
2DG
2DG + DPR

Figure 18 DPR Inhibits Purine Release as provoked by 2-DG Treatment and Inosine is the Primary Released Nucleoside

*WT and transfected HEK293T cells were grown to 80% confluence in 12 well culture plates and pretreated with [^{3}H]adenine for 30 min at 37°C. Cells were treated with 2-DG to induce cellular purine nucleoside release in comparison to DPR treated cells. Collected extracellular samples were combined with a cold carrier to assess nucleoside release by TLC separation on gel-silica plates. Individual purines were collected and radioactivity was measured by scintillation spectrometry. Data expressed as N of 2 with experiments performed in quadruplicate and results were assessed by t-test whereby * indicates significance $p < 0.05$. It was found that inosine was the primary nucleoside released by 2-DG (A and B) and no cell-type difference was observed.*

WT cells: A-inosine release; C-adenosine release; E-hypoxanthine release

Transfected cells: B-inosine release; D-adenosine release; F-hypoxanthine release

Chapter 5

Discussion & Future Directions

5.1 Restatement of research question

Both in terms of function and expression, ENT3 remains a poorly understood transporter. Current consensus suggests ENT3 to be a pH-dependent, intracellular transporter, localised primarily on lysosomal and mitochondrial membranes. Although substrate specificity of ENT3 remains to be determined it is thought to be a broad spectrum transporter mainly involved in nucleoside salvage pathways. Tissue distribution studies, based solely on mRNA levels, have shown ENT3 to be ubiquitously expressed throughout the body.

The present study was conducted to investigate ENT3 within brain with an emphasis on the role of ENT3 in adenosine signaling pathways. Although the signaling properties of adenosine have been well characterized, demonstrating numerous and diverse processes within the CNS that are regulated via adenosine, the mechanisms involved in regulating adenosine concentrations remain poorly understood. Until recently ENT1, ENT2 and ecto-5'-nucleotidases were thought to be the most important components in regulating extracellular adenosine concentrations however, it is now accepted that the activity of these three

proteins does not fully explain our observations of adenosine regulation. As a result, researchers have turned their attention to the more recently identified and less known ENT isoforms, ENT3 and ENT4, as they may play a yet unexplored role in adenosine signaling.

In hopes of determining the functional role of ENT3 we first sought to determine *in vivo* localisation. Studies of the brain were conducted using numerous methods including RT-PCR, western blot analysis and immunocytochemistry (ICC). By using a combination of techniques, rather than relying on one, we were able to confirm our findings and increase confidence in our findings. Studies were conducted with isolated brain regions from CD1 mice, primary cell cultures harvested from mouse brain and cellular components isolated from mice cortex and cerebellum by differential centrifugation to present a complete picture of the *in vivo* localisation of ENT3.

As ENT3 is a novel transporter, studies were initially problematic as there are very few antibodies targeting ENT3 and those that are commercially available lack experimental data validating antibody specificity. Despite this, we were able to assess and select a highly specific commercial antiENT3 antibody by creating a flag-tagged mENT3 protein; commercial antibody specificity was confirmed by comparing band sizes to that of an antibody specific to the flag epitope by western blot analysis. This antibody was then used for all subsequent experiments as our data indicated that it was specific for ENT3.

By isolating brain regions, cortex, cerebellum, striatum and hippocampus, from CD1 mice we have shown ENT3 to be ubiquitously expressed throughout brain by both Rt-PCR and western blot analysis. Rt-PCR of primary neurons and astrocytes showed ENT3 expression and western blot analysis confirmed ENT3 in neurons and astrocytes but not in microglia. ICC of neurons and astrocytes indicate ENT3 to be intracellularly localised. To

confirm cellular localisation of ENT3, isolated cortex and cerebellum were subjected to differential centrifugation, which separated tissue samples into fractions dependent on their size and density. Our western blot analysis of isolated fractions indicated ENT3 protein was found within the cytosolic fraction.

5.2 Comparison to the current literature

Conducting a simple search of ENT3 in the current literature will quickly reveal that there are very few papers available on ENT3 specifically and those that have been published remain incomplete for a variety of reasons. Our work was not intended to complete previously conducted studies but to stand as an independent study, presenting the most complete picture of ENT3 localisation in brain as possible.

The majority of studies rely solely on Rt-PCR whereby ENT3 expression is determined by isolating RNA from specific samples. Although Rt-PCR is a widely used technique, RNA levels do not necessary reflect protein abundance and therefore Rt-PCR should always be complimented with other means of detection. Isolated neurons and astrocytes have previously been shown to express ENT3 by Rt-PCR only (Li et al., 2013). Albeit, an important first step, Rt-PCR offers little to no information on the protein abundance or localisation nor insight as to the activity level of ENT3.

Accordingly, we sought to characterize ENT3 expression of both neurons and astrocytes, in addition to microglia cells and bEND3 cells, but by using multiple techniques to collect as much information as possible. Neurons and astrocytes were initially tested by Rt-PCR, and were determined to be positive for ENT3 mRNA expression as a single PCR

product was obtained of the expected size of 245bp. To compliment Rt-PCR experiments, western blot analysis was performed using protein collected from primary cells: neurons, astrocytes and microglia. As well protein was harvested from bEND3 cells, an immortalized mouse endothelial cell line, as a means of assessing endothelial cells for ENT3 expression. Endothelial cells were assessed for ENT3 expression as they are considered the principal barrier separating microcirculation and surrounding tissue. The expression of NTs is of utmost importance to permit the uptake and release of nucleosides to maintain normal physiological processes. Western blot analysis confirmed ENT3 protein expression in both neurons and astrocytes but not in microglia or bEND3 cells.

ICC was performed as an additional means of examining ENT3 expression and localisation in neurons and astrocytes. Cells were stained with ENT3(N-20) antibody and the corresponding fluorescent conjugated secondary antibody and images were visualized using a fluorescence microscope. ICC results confirmed intracellular localisation of ENT3 protein, as fluorescence of both neurons and astrocytes was found contained within the cytoplasm of both cell types. Although previous studies have demonstrated neurons and astrocytes to express ENT3, by using a combination of methods as described here briefly, our studies have gone beyond those of other groups to demonstrate with conviction that neurons and astrocytes express ENT3 protein. It should be noted that although cells were primary cell cultures, harvested from CD1 mice, culturing cells *in vitro* could induce unknown and unexpected changes in protein expression and therefore our findings may not reflect *in vivo* cells.

Previously, male and female mice and rats were assessed for tissue distribution of ENT3 by Rt-PCR; using whole brain homogenates and both species were determined to be

positive for ENT3 expression (Lu et al., 2004). For our studies we chose to use male mouse brain only whereby CD1 mice were dissected to isolate brain regions of interest, cortex, cerebellum, striatum and hippocampus, and analysed by Rt-PCR and western blot to determine endogenous ENT3 expression more accurately. Each region was found to test positive for both ENT3 mRNA, indicated by the presence of a single PCR product at the expected band size, and protein, by the presence of a band at 52 kD. Comparing protein expression of each brain region by western blot analysis suggests ENT3 to be expressed at relatively equal levels throughout brain.

Recent studies have indicated ENT3 to be primarily an intracellular transporter, localised on lysosomes, endosomes and mitochondrial membranes (Baldwin et al., 2005; Govindarajan et al., 2009; Hsu et al., 2012). In stark contrast to other members of the ENT family, ENT3 gene sequence was found to possess a 51-residue hydrophilic N-terminal region, which contains motifs similar to those known to be involved in intracellular trafficking processes (Hyde et al., 2001). The discovery of this N-terminal region was the first indication that ENT3 could be an intracellular transporter but since its discovery studies have been published confirming hENT3 to be localised to intracellular membranes (Baldwin et al., 2005), within mitochondria (Govindarajan et al., 2009) and vital to lysosomal function within macrophages (Hsu et al., 2012).

To complicate matters further, localisation of ENT3 has been suggested to be cell type dependent by multiple sources. The Govindarajan group published a study in 2008 which examined multiple human cell lines to assess the expression and the localisation of hENT3 by western blot analysis and immunostaining. The cell lines included in the study originated from a variety of human tissues including placenta (JAR, BeWo and JEG3), cervical

epithelium (HeLa), breast (MDA-MB-231, Mcf-10A), ovary (Sk-0v-3) and liver (HepG2), all of which showed similar levels of expression of hENT3 protein (Govindarajan et al., 2009). Western blot analysis was combined with immunolocalisation studies of the same human cell lines which showed distinct distribution patterns of hENT3 that varied between different cell lines. Staining, using an in-house generated rabbit polyclonal antibody, was found to be primarily cell surface in placenta, cytosolic in breast and cervical cells and a combination of vesicular and mixed patterns were seen in ovarian and liver cells (Govindarajan et al., 2009).

Although our findings have confirmed ENT3 to be primarily an intracellular transporter, neither immunostaining of brain cells nor differential centrifugation of brain tissues have been indicative of mitochondrial localisation of ENT3. ICC of both astrocytes and neurons suggests intracellular localisation, which was further explored by separating cell components by differential centrifugation based on density and size, into four separate fractions; nuclear, mitochondrial, plasma membrane and cytosolic. These samples were then separated and probed for ENT3 expression by western blot analysis which found high abundance of ENT3 within the cytosolic fraction and not the mitochondrial fraction as was expected.

This is not to say that ENT3 cannot be localised to such intracellular organelles as the mitochondria or lysosomes but that further studies, specific to brain, are needed to determine the precise localisation of ENT3. The most complete study of ENT3 localisation to date did not include any human brain cell lines but as distribution of ENT3 was shown to vary among those cell lines tested, it is reasonable to assume that hENT3 localisation within

brain could be different from that seen in cells of tissues outside the CNS and as such should be assessed specifically (Govindarajan et al., 2009).

Furthermore, western blot analysis of the subcellular fractions isolated from brain tissue using the ENT3(N-20) antibody revealed a smaller than expected band, of 30kD, within the mitochondrial fraction. It is possible that this smaller protein could be a yet unidentified functional splice variant of ENT3 localised to the mitochondrial membrane. In addition, the cytosolic fraction contains all cellular components that were not pelleted by previous spin cycles, which may include small lysosomes or vesicular carriers. These cellular components could be the source of ENT3 and therefore further characterization of the cytosolic fraction is warranted.

To assess ENT3 activity, functional assays were performed using WT and mENT3-Flag transfected HEK293T cells. Cells were treated with 2-DG to provoke purine release and compared to DPR, an inhibitor of ENT1 and ENT2, treated cells. No cell-type differences were observed as DPR was demonstrated to be similarly effective at inhibiting purine release and inosine, identified by TLC separation, was the primary nucleoside released by 2-DG treatment in both cell types. Our functional assays were performed at physiological pH and as current literature suggests ENT3 activity to be pH dependent, with optimal activity at pH 5.5-6.5 (Baldwin et al., 2005; Govindarajan et al., 2009), the lack of cell-type difference in such conditions could be due to minimal ENT3 activity at the higher pH. Repeating similar functional assays while varying the pH conditions may result in widely different outcomes.

5.3 Explanation of unexpected findings

As ENT3 is an understudied transporter there is much need for in-depth studies, such as ours, to elucidate the localisation, function and substrate specificity of this novel ENT subtype. These studies were limited by the paucity of tools, such as specific commercial antibodies, which are required to study ENT3.

In the present study we first sought to assess available commercial antibodies targeting ENT3. To do so, the mouse ENT3 cDNA sequence was inserted into a pIRES-puro-Flag plasmid and transfected into HEK293T cells, to express the mENT3 protein with a flag epitope located on the N-terminus. AntiENT3 antibodies were compared to an antibody targeting the flag epitope by western blot analysis to evaluate specificity; these results were not as expected. Using the ENT3(N-20) antibody, transfected HEK293T cells showed three bands of 40, 75 and 150 kD which is in contrast to expected results of a single band of 52 kD as indicated by the company, Santa Cruz Biotechnologies, and based on the size predicted by the sequence.

There are a number of hypotheses to explain why the transfected HEK293T cells are not expressing mENT3 at the expected size. One possibility is that the flag-tag sequence, attached to the N-terminus of the mENT3 gene disrupts the normal trafficking processes; the endogenous N-terminal region is thought to direct the ENT3 protein to the lysosomes, based on sequence comparisons to other known proteins (Bonifacino and Traub, 2003). Alterations in protein trafficking could result in abnormal protein processing or aggregation that could explain the unanticipated band sizes. A study was performed in which the hENT1 and mENT1 cDNA was inserted into the p3xFLAG-CMV-7.1 plasmid to evaluate

ENT1 function; western blot analysis of transfected cells demonstrated larger than expected bands indicating a greater tendency of transfected proteins to aggregate as well as their resistance to denaturing conditions (Reyes et al., 2010). This could also be the case for our pIRES-puro-flag-mENT3 plasmid.

Another possibility is that the transfected HEK293T cells are not able to correctly process the mouse ENT3 protein encoded by the transfected pIRES-puro-Flag-mENT3 plasmid. Western blot analysis revealing proteins that are larger than anticipated can be due to various protein modifications, such as glycosylation, which would increase their molecular weight. Proteins that are smaller than expected could be due to activation of degradation pathways that do not recognize the exogenous protein. Although the observed band sizes of the ENT3-flag protein expressed in transfected HEK293T cells were abnormal, the 40kDa band is perhaps not entirely unexpected as another group that had created a N-terminal YFP-tagged hENT3 protein transfected into HeLa cells also showed a secondary band of approximately 40kDa (Govindarajan et al., 2009). While the multiple bands and unexpected band sizes were of interest, the primary ENT3 antibody validation rested on western blot analysis that showed that there were protein bands labelled by both an antibody targeting the flag epitope and the ENT3(N-20) commercial antibody.

In addition to using transfected HEK293T cells for assessing commercial ENT3 antibodies, we had hoped an established stable transfected HEK293T cell line could be used for functional assays. As transfected cells would have an increased expression of ENT3, assays comparing transfected to WT cells could be conducted offering insight as to the role of ENT3 in adenosine transport. Although we were skeptical to conduct functional assays using the transfected HEK cells based on the unexpected western blot results described

above, one assay was designed in which control cells were compared to cells deprived of glucose, by substituting glucose with 2-DG, and those deprived of glucose in combination with DPR. Total purine release was measured by scintillation spectrometry and results were assessed by one-way ANOVA indicating a significant difference in total purine release in control groups as compared to 2-DG treated in both WT and transfected cells. Contrary to our initial hypothesis, that the transfected cells would be less affected by DPR treatment, WT cells showed greater total purine release. TLC separation was subsequently performed to determine the specific effect of DPR treatment on purines released. Results were assessed by t-test and indicated inosine to be the most abundantly released purine as provoked by 2-DG and release was significantly inhibited by DPR, as has been previously demonstrated (Phillis et al., 1989). Subsequent functional assays using the mENT3-Flag transfected HEK293T cells were not performed as we were not confident that the transfected mENT3 protein retained its physiological function and would be representative of endogenous ENT3 within brain.

As we had demonstrated that the chosen commercial ENT3(N-20) antibody was of high specificity, western blot analysis was then performed using isolated mouse brain regions. Repeated experiments consistently showed two bands for each brain region tested. One band was of the expected size of 52 kD confirming ENT3 protein expression throughout brain and a second, the unexpected band, was found at 30 kD. A similar band of 30 kD was also found by western blot analysis of mouse cortical astrocytes and was in fact stronger than that of the expected 52 kD band. It may be that the 30 kD protein consistently identified by western blot is an ENT3 variant, primarily expressed within astrocytes, which would explain its presence within total brain homogenants. It is worth noting that mouse

hippocampal neurons were also probed for ENT3 expression by western blot analysis and consistently showed one sole band of 52 kD. This indicates that the ENT3(N-20) antibody is not recognizing a 30 kD protein in all samples.

Western blot analysis of subcellular fractionation samples, separated from mouse cortex and cerebellum into nuclear, mitochondrial, plasma membrane and cytosolic fractions, showed a strong signal for ENT3 within the cytosolic fraction only at the expected size of 52 kD. As it has already been stated, ENT3 is currently thought to be expressed on the mitochondrial or lysosomal membranes (Baldwin et al., 2005; Govindarajan et al., 2009). It should be noted that both the mitochondrial and plasma membrane fraction showed no band at 52 kD but had a weak band at 30 kD. The persistence of a band for ENT3 at 30 kD is intriguing; further studies are needed to assess this smaller protein recognized by the ENT3 antibody. Our conclusion that full length ENT3 is largely restricted to cytosol, would benefit from additional western blotting studies to identify proteins, and by extension, cellular components included in this final fraction, which could indicate the subcellular localisation of ENT3.

It should be noted that although the differential centrifugation protocol was followed closely, several factors could influence the outcome. The composition of the subcellular fractionation buffer plays a key role in the fractionation of cellular components. Biological detergents, also known as surfactants, act by solubilizing cell membranes to release intracellular components. There are two principal types of detergents: ionic detergents, which are harsher detergents that denature proteins and disrupt molecular interactions, such as protein-protein and protein-lipid and milder, non-ionic detergents, which do not denature proteins or disrupt protein-protein interactions. Our buffer, composed of sucrose, HEPES,

KCl, $MgCl_2$ (Fisher Scientific), EDTA and EGTA, should not affect protein structure or protein interactions and the combined action of EDTA and EGTA, two chelating agents, should be sufficient to sequester any ions present.

Our studies have primarily concentrated on investigating ENT3 expression within neurons and astrocytes although microglia and bEND3 cell lysate was harvested and subjected to western blot analysis, along with neurons and astrocytes, as a preliminary assessment of ENT3 protein expression. Neither microglia nor bEND3 cells were found to express ENT3. It is important to note that lack of a positive result from western blot analysis could be due to insufficient protein loaded or due to ENT3 not being fully extracted from cells, which could be the case for cells homogenized directly in loading buffer rather than a lysis buffer. There are a number of lysis buffers that can be used to prepare samples for running on a gel. These buffers differ in their ability to disrupt cell membranes, solubilize intracellular components and release proteins of interest. Lysis buffers containing ionic detergents are the harshest buffers and usually yield the highest protein levels. Optimization, to determine the most effective lysis buffer and the ideal temperature to denature our protein of interest was assessed by repeating western blots under various conditions. As such it was determined that NP-40 buffer enabled sufficient protein yield and was used to prepare and lyse cell and tissue samples. However, microglia and bEND3 cells were lysed in gel loading buffer and not in NP-40 buffer because this two-step procedure would have diluted our protein samples beyond a workable concentration.

Previous studies have demonstrated ENT3 to have an important role in maintaining lysosome function within macrophages (Hsu et al., 2012). Macrophages are the phagocytic cells of the immune system meaning they are responsible for the uptake and breakdown of

unwanted, circulating cells and particles. The majority of degradation by macrophages is performed within lysosomes and consequently represents a major source of nucleoside recycling from the breakdown of nucleic acids of phagocytosed cells. Characterization of macrophages has found ENT3 to be the highest expressed of all ENT isoforms (Hsu et al., 2012). As a result of this initial observation, an ENT3 knockout mouse model was generated by Hsu et al and used to investigate the functional *in vivo* role of ENT3 which was found to be a vital lysosomal transporter, regulating nucleoside trafficking and maintaining lysosomal integrity (Hsu et al., 2012). Further studies exploring ENT3 expression within microglia are of interest as microglia cells are the immune cells of the CNS and could therefore, like macrophages, rely similarly on ENT3 to maintain lysosome integrity.

ICC was performed with hippocampal neurons and cortical astrocytes harvested from CD1 mice and we were able to detect a fluorescent signal in both cell types indicating intracellular expression of ENT3. The ENT3(N-20) antibody used for all ICC experiments was found to have a relatively low signal for ICC, which required a high working concentration of both primary and secondary antibodies. As a result, there was a high background signal, however, specificity was confirmed through the use of no primary control slides.
It is possible that ICC studies may be improved by further optimization of the experimental procedure. Cold methanol was chosen as fixative but other options are available and could be tried such as 4% paraformaldehyde or acetone. As some epitope structures are altered upon exposure to methanol, antibody affinity may be compromised and could influence results. Including an additional amplification step may also be beneficial; as ENT3 may not be abundantly expressed in certain cell types, an amplification procedure, such as the

use of a biotinylated secondary antibody and streptavidin-conjugated to a fluorophor, may improve the detection of ENT3.

ICC images were collected using an Olympus IX51 fluorescent microscope, generously donated by Dr. Don Miller (University of Manitoba, Winnipeg, Manitoba) and although this system allowed us to have some success in visualizing stained cells ideally we would like to revisit cell staining using a confocal microscope that could generate images of higher resolution and quality by collecting a plane of focus and do to lasers of precise excitations lines, which would eliminate overlap in fluorescent emissions.

5.4 Major conclusions from study

Our main findings indicate ENT3 to be ubiquitously expressed throughout brain. Using a number of methods, we identified ENT3 within cortex, cerebellum, striatum and hippocampus of mouse brain. To our knowledge, ENT3 expression within brain regions by western blot analysis has not been previously demonstrated. In addition, ENT3 was found expressed in neurons as well as in astrocytes but not in microglia cultures and based on both ICC of primary cell and subcellular fractionation, ENT3 was determined to be localised primarily within the cytosol. Although we have not yet been able to elucidate the functional activity of ENT3, our findings of the localisation of ENT3 within brain are the first step in understanding this transporter.

As a member of the ENT family, researchers may be interested in the capacity of ENT3 to transport adenosine and the role of ENT3 in adenosine signaling within brain. To date ENT1 and ENT2 have been best characterized. As they are abundantly expressed on

plasma membranes, ENT 1 and 2 are considered the principal transporters involved in adenosine signaling. By regulating extracellular adenosine concentration they control the availability of adenosine to act on corresponding cell surface receptors. In contrast, ENT3 is not considered directly responsible for adenosine signalling pathways as it is found primarily within cells. However, ENT3 may still play important roles in regulating adenosine signaling by influencing the intracellular nucleoside pools; ENT3 activity could dictate the amount of adenosine available for release by ENT1 and 2. In addition, ENT3 could have a novel function in adenosine signaling. Although previously discounted, recent studies have indicated adenosine can be stored in synaptic vesicles and secretory granules and can be released by exocytosis (Corti et al., 2013; Klyuch et al., 2012). Although questions still remain, ENT3 could be responsible for transporting adenosine across vesicle or granule membranes, using the proton gradient, where it could be stored until needed for release and initiation of signaling cascades.

ENT3 is the only subtype of the ENT family found to be associated with human disorders. Mutations in the *SLC29A3* gene have been linked to syndromes including H syndrome, familial histiocytosis syndrome and familial Rosai-Dorfman disease (Cliffe et al., 2009; Huber-Ruano et al., 2012; Morgan et al., 2010). The four subtypes of the ENT family have been shown to overlap, in terms of substrate specificity and cell-type distribution, yet only mutations within the ENT3 gene have been identified to result in human disorders, which suggests ENT3 has a unique role *in vivo*.

Studies of individuals who possess at least one mutation within the hENT3 gene sequence were compiled to assess the physiological function of hENT3 (Hiller et al., 2013; Kang et al., 2010). Unfortunately, such studies are complex as multiple mutations have

been identified and the human disorders are of varying severity and a variety of clinical phenotypes. Nevertheless, many of the symptoms of disorders related to SLC29A3 gene mutations have been linked to mitochondrial malfunctions including short stature and hearing loss (Kang et al., 2010). In some cases, ENT3 gene mutations were associated with changes in mitochondrial nucleotide pools, altered mitochondrial DNA synthesis and altered oxidative phosphorylation, indicating an important role of ENT3 in mitochondrial function (DiMauro and Schon, 2001; Kang et al., 2010). Other common symptoms include histiocytosis, an excessive number of tissue macrophages, and enlarged or abnormal lymph nodes (Huber-Ruano et al., 2012); as histiocytes are incapable of de novo nucleotide synthesis, salvage pathways that rely on ENT3 to retain nucleosides produced by degradation processes, are of critical importance and indicate an important role of ENT3 localised on lysosomes. Although hENT3 mutations are multisystemic, the majority of symptoms are concentrated to the trunk and lower limbs and function of the CNS seems to be less affected. However in some cases mental retardation can develop due to *SLC29A3* mutations and is thought to be caused by mitochondrial respiratory chain defects, again supporting hENT3 localisation within mitochondria.

There are a number of therapeutic implications related to the ENT family, and in particular ENT3, as they are responsible for the flux of therapeutic agents such as NADs. To enter the target cell, where they are phosphorylated to their active nucleotide derivatives, NADs must first be transported across the cell membrane. This is particularly true of ENT1 and 2, which are located on plasma membranes. ENT3 present on mitochondrial membranes could contribute to the accumulation of antiviral and anticancer therapeutic agents within the mitochondria and could result in cytotoxicity, a side effect often associated with

NADs (Govindarajan et al., 2009). A more complete understanding of localisation and function of ENT3 would allow us to understand the toxicities of certain drugs and even potentially modulate the activity of ENT3; co-administration of an ENT3 inhibitor could allow patients to benefit from therapy for longer as toxic accumulation of these therapeutic agents would be minimized.

5.5 Future Directions

Current literature has demonstrated ENT3 to be an intracellular transporter, with a few unique properties as compared to other members of the ENT family. Although we have attempted to identify localisation of ENT3 within brain, further studies are needed. As mentioned previously, studies of ENT3 are limited. Until recently, the role of ENT3 in signaling pathways was thought to be insubstantial, given its intracellular localisation. However as the mechanisms involved in regulating extracellular adenosine concentrations remain incompletely characterized, researchers have sought out ENT3 as a potential answer to lingering questions. As more labs become interested in ENT3 research the availability of appropriate and high quality tools, such as commercial antibodies, selective inhibitors and characteristic permeants, will improve.

For our studies we created a pIRES-puro-Flag plasmid containing the mENT3 gene sequence to allow validation of commercial antiENT3 antibodies that currently lack experimental data. It was important to assess and confirm all commercial antibodies prior to

conducting any experiments. This information will benefit future researchers that can design and conduct further studies of ENT3, using the same commercial antibody we have validated, with the knowledge that it is of high specificity for the ENT3 protein.

Although we have attempted to assess localisation of ENT3 within brain, further studies should be conducted to replicate and extend our findings. Our work has demonstrated ENT3 to be ubiquitously expressed through brain but attempts to investigate the intracellular localisation, using both tissue samples and primary cell cultures, have confirmed only that ENT3 is found within the cytosol. Other groups have attempted to determine localisation of ENT3 with mixed success (Govindarajan et al., 2009). Current literature indicates ENT3 to be expressed primarily in mitochondrial and lysosomal membranes and involved in nucleoside salvage pathways (Baldwin et al., 2005; Govindarajan et al., 2009; Hsu et al., 2012). Reported differences in ENT3 localisation may indicate cell-type dependent localisation or may be a consequence of the use of fusion proteins (Baldwin et al., 2005; Govindarajan et al., 2009). In the present study, we were unable to isolate ENT3 within mitochondria of brain samples. Improving subcellular isolation techniques, perhaps performing differential centrifugation with density gradients or further ICC studies with a three step protocol could improve upon our current findings and offer information as to the endogenous function of ENT3 within brain.

The functional role of ENT3 in terms of its contribution to adenosine signaling needs further characterization. A cell line stably transfected with a native form of ENT3 (lacking any additional tags or epitopes or fusion proteins) may be an appropriate tool. A high level of expression may allow improved localisation by ICC and/or cell fractionation. Alternatively, using siRNA to knockdown endogenous ENT3 expression in HEK293T cells, or

another cell line, may offer a good cell model system to assess ENT3 function. in comparison to WT cells.

As ENT3 is an intracellular transporter, establishing functional assays of adenosine translocation is difficult. Although ENT3 has been suggested to be pH dependent, with greatest activity demonstrated between pH 6.5-5.5 (Baldwin et al., 2005; Govindarajan et al., 2009), alterations to the extracellular pH would mostly likely not influence the activity of ENT3. An alternative would be to disrupt the normal pH of organelles, such as mitochondria or lysosomes specifically, to assess the effects of such alterations on ENT3 activity. Functional assays could also be conducted in the presence of ENT1 and ENT2 inhibitors in order to demonstrate the specific activity of ENT3, in addition under the same circumstances we could investigate the possibility of a compensatory response by ENT3 when ENT1 and 2 are blocked. Finally, assays with certain NADs, in transfected cell lines overexpressing ENT3 could indicate if ENT3 is involved in cytotoxicity following drug administration; this could demonstrate ENT3 localisation and also offer insight to substrate selectivity.

Although discovered almost fifteen years ago (Hyde et al., 2001), studies on ENT3 remain limited due primarily to the lack of appropriate and selective tools. Furthermore, ENT3 has been suggested to be an intracellular transporter and was thought to not be directly involved in adenosine signaling pathways. However understanding adenosine signaling requires studies of both extracellular and intracellular pathways. ENT3, ubiquitously expressed throughout brain, has the potential to be a vital component in regulating adenosine levels in both physiological and pathophysiological conditions.

Bibliography

Acimovic, Y., and Coe, I.R. (2002). Molecular evolution of the equilibrative nucleoside transporter family: identification of novel family members in prokaryotes and eukaryotes. Molecular biology and evolution *19*, 2199-2210.

Armstrong, D., Summers, C., Ewart, L., Nylander, S., Sidaway, J.E., and van Giezen, J.J. (2014). Characterization of the adenosine pharmacology of ticagrelor reveals therapeutically relevant inhibition of equilibrative nucleoside transporter 1. Journal of cardiovascular pharmacology and therapeutics *19*, 209-219.

Azuma, A., Huang, P., Matsuda, A., and Plunkett, W. (2001). 2'-C-cyano-2'-deoxy-1-beta-D-arabino-pentofuranosylcytosine: a novel anticancer nucleoside analog that causes both DNA strand breaks and G(2) arrest. Molecular pharmacology *59*, 725-731.

Bachmann, H.S., Siffert, W., and Frey, U.H. (2003). Successful amplification of extremely GC-rich promoter regions using a novel 'slowdown PCR' technique. Pharmacogenetics *13*, 759-766.

Baldwin, S.A., Beal, P.R., Yao, S.Y., King, A.E., Cass, C.E., and Young, J.D. (2004). The equilibrative nucleoside transporter family, SLC29. Pflugers Archiv : European journal of physiology *447*, 735-743.

Baldwin, S.A., Mackey, J.R., Cass, C.E., and Young, J.D. (1999). Nucleoside transporters: molecular biology and implications for therapeutic development. Molecular medicine today *5*, 216-224.

Baldwin, S.A., Yao, S.Y., Hyde, R.J., Ng, A.M., Foppolo, S., Barnes, K., Ritzel, M.W., Cass, C.E., and Young, J.D. (2005). Functional characterization of novel human and mouse

equilibrative nucleoside transporters (hENT3 and mENT3) located in intracellular membranes. The Journal of biological chemistry *280*, 15880-15887.

Barnes, K., Dobrzynski, H., Foppolo, S., Beal, P.R., Ismat, F., Scullion, E.R., Sun, L., Tellez, J., Ritzel, M.W., Claycomb, W.C., *et al.* (2006). Distribution and functional characterization of equilibrative nucleoside transporter-4, a novel cardiac adenosine transporter activated at acidic pH. Circulation research *99*, 510-519.

Bonifacino, J.S., and Traub, L.M. (2003). Signals for sorting of transmembrane proteins to endosomes and lysosomes. Annual review of biochemistry *72*, 395-447.

Brand, A., Vissiennon, Z., Eschke, D., and Nieber, K. (2001). Adenosine A(1) and A(3) receptors mediate inhibition of synaptic transmission in rat cortical neurons. Neuropharmacology *40*, 85-95.

Brundege, J.M., and Dunwiddie, T.V. (1998). Metabolic regulation of endogenous adenosine release from single neurons. Neuroreport *9*, 3007-3011.

Burnstock, G. (1972). Purinergic nerves. Pharmacological reviews *24*, 509-581.

Chen, J., Rinaldo, L., Lim, S.J., Young, H., Messing, R.O., and Choi, D.S. (2007). The type 1 equilibrative nucleoside transporter regulates anxiety-like behavior in mice. Genes, brain, and behavior *6*, 776-783.

Choi, D.S., Cascini, M.G., Mailliard, W., Young, H., Paredes, P., McMahon, T., Diamond, I., Bonci, A., and Messing, R.O. (2004). The type 1 equilibrative nucleoside transporter regulates ethanol intoxication and preference. Nature neuroscience *7*, 855-861.

Cliffe, S.T., Kramer, J.M., Hussain, K., Robben, J.H., de Jong, E.K., de Brouwer, A.P., Nibbeling, E., Kamsteeg, E.J., Wong, M., Prendiville, J., *et al.* (2009). SLC29A3 gene is mutated in pigmented hypertrichosis with insulin-dependent diabetes mellitus syndrome and interacts with the insulin signaling pathway. Human molecular genetics *18*, 2257-2265.

Correia-de-Sa, P., Timoteo, M.A., and Ribeiro, J.A. (1996). Presynaptic A1 inhibitory/A2A facilitatory adenosine receptor activation balance depends on motor nerve stimulation paradigm at the rat hemidiaphragm. Journal of neurophysiology *76*, 3910-3919.

Corti, F., Cellai, L., Melani, A., Donati, C., Bruni, P., and Pedata, F. (2013). Adenosine is present in rat brain synaptic vesicles. Neuroreport *24*, 982-987.

Crawford, C.R., Patel, D.H., Naeve, C., and Belt, J.A. (1998). Cloning of the human equilibrative, nitrobenzylmercaptopurine riboside (NBMPR)-insensitive nucleoside transporter ei by functional expression in a transport-deficient cell line. The Journal of biological chemistry *273*, 5288-5293.

Cunha, R.A. (2005). Neuroprotection by adenosine in the brain: From A(1) receptor activation to A (2A) receptor blockade. Purinergic signalling *1*, 111-134.

Cunha, R.A., Milusheva, E., Vizi, E.S., Ribeiro, J.A., and Sebastiao, A.M. (1994). Excitatory and inhibitory effects of A1 and A2A adenosine receptor activation on the electrically evoked [3H]acetylcholine release from different areas of the rat hippocampus. Journal of neurochemistry *63*, 207-214.

Damaraju, V.L., Damaraju, S., Young, J.D., Baldwin, S.A., Mackey, J., Sawyer, M.B., and Cass, C.E. (2003). Nucleoside anticancer drugs: the role of nucleoside transporters in resistance to cancer chemotherapy. Oncogene *22*, 7524-7536.

de Jesus, J., Imane, Z., Senee, V., Romero, S., Guillausseau, P.J., Balafrej, A., and Julier, C. (2013). SLC29A3 mutation in a patient with syndromic diabetes with features of pigmented hypertrichotic dermatosis with insulin-dependent diabetes, H syndrome and Faisalabad histiocytosis. Diabetes & metabolism *39*, 281-285.

DeLander, G.E., and Hopkins, C.J. (1986). Spinal adenosine modulates descending antinociceptive pathways stimulated by morphine. The Journal of pharmacology and experimental therapeutics *239*, 88-93.

DiMauro, S., and Schon, E.A. (2001). Mitochondrial DNA mutations in human disease. American journal of medical genetics *106*, 18-26.

Drury, A.N., and Szent-Gyorgyi, A. (1929). The physiological activity of adenine compounds with especial reference to their action upon the mammalian heart. The Journal of physiology *68*, 213-237.

Dunwiddie, T.V. (1999). Adenosine and suppression of seizures. Advances in neurology *79*, 1001-1010.

Dunwiddie, T.V., and Masino, S.A. (2001). The role and regulation of adenosine in the central nervous system. Annual review of neuroscience *24*, 31-55.

Elbarbary, N.S., Tjora, E., Molnes, J., Lie, B.A., Habib, M.A., Salem, M.A., and Njolstad, P.R. (2013). An Egyptian family with H syndrome due to a novel mutation in SLC29A3 illustrating overlapping features with pigmented hypertrichotic dermatosis with insulin-dependent diabetes and Faisalabad histiocytosis. Pediatric diabetes *14*, 466-472.

Engel, K., Zhou, M., and Wang, J. (2004). Identification and characterization of a novel monoamine transporter in the human brain. The Journal of biological chemistry *279*, 50042-50049.

Farooq, M., Moustafa, R.M., Fujimoto, A., Fujikawa, H., Abbas, O., Kibbi, A.G., Kurban, M., and Shimomura, Y. (2012). Identification of two novel mutations in SLC29A3 encoding an equilibrative nucleoside transporter (hENT3) in two distinct Syrian families with H syndrome: expression studies of SLC29A3 (hENT3) in human skin. Dermatology *224*, 277-284.

Fredholm, B.B., AP, I.J., Jacobson, K.A., Klotz, K.N., and Linden, J. (2001). International Union of Pharmacology. XXV. Nomenclature and classification of adenosine receptors. Pharmacological reviews *53*, 527-552.

Frenguelli, B.G., Wigmore, G., Llaudet, E., and Dale, N. (2007). Temporal and mechanistic dissociation of ATP and adenosine release during ischaemia in the mammalian hippocampus. Journal of neurochemistry *101*, 1400-1413.

Gouder, N., Scheurer, L., Fritschy, J.M., and Boison, D. (2004). Overexpression of adenosine kinase in epileptic hippocampus contributes to epileptogenesis. The Journal of neuroscience : the official journal of the Society for Neuroscience *24*, 692-701.

Govindarajan, R., Leung, G.P., Zhou, M., Tse, C.M., Wang, J., and Unadkat, J.D. (2009). Facilitated mitochondrial import of antiviral and anticancer nucleoside drugs by human equilibrative nucleoside transporter-3. American journal of physiology Gastrointestinal and liver physiology *296*, G910-922.

Gray, J.H., Owen, R.P., and Giacomini, K.M. (2004). The concentrative nucleoside transporter family, SLC28. Pflugers Archiv : European journal of physiology *447*, 728-734.

Griffith, D.A., and Jarvis, S.M. (1996). Nucleoside and nucleobase transport systems of mammalian cells. Biochimica et biophysica acta *1286*, 153-181.

Griffiths, M., Beaumont, N., Yao, S.Y., Sundaram, M., Boumah, C.E., Davies, A., Kwong, F.Y., Coe, I., Cass, C.E., Young, J.D., *et al.* (1997). Cloning of a human nucleoside transporter implicated in the cellular uptake of adenosine and chemotherapeutic drugs. Nature medicine *3*, 89-93.

Haystead, T.A. (2006). The purinome, a complex mix of drug and toxicity targets. Current topics in medicinal chemistry *6*, 1117-1127.

Hiller, N., Zlotogorski, A., Simanovsky, N., Ingber, A., Ramot, Y., and Molho-Pessach, V. (2013). The spectrum of radiological findings in H syndrome. Clinical imaging *37*, 313-319.

Hsu, C.L., Lin, W., Seshasayee, D., Chen, Y.H., Ding, X., Lin, Z., Suto, E., Huang, Z., Lee, W.P., Park, H., *et al.* (2012). Equilibrative nucleoside transporter 3 deficiency perturbs lysosome function and macrophage homeostasis. Science *335*, 89-92.

Huber-Ruano, I., Errasti-Murugarren, E., Godoy, V., Vera, A., Andreu, A.L., Garcia-Arumi, E., Marti, R., and Pastor-Anglada, M. (2012). Functional outcome of a novel SLC29A3 mutation identified in a patient with H syndrome. Biochemical and biophysical research communications *428*, 532-537.

Huston, J.P., Haas, H.L., Boix, F., Pfister, M., Decking, U., Schrader, J., and Schwarting, R.K. (1996). Extracellular adenosine levels in neostriatum and hippocampus during rest and activity periods of rats. Neuroscience *73*, 99-107.

Hyde, R.J., Cass, C.E., Young, J.D., and Baldwin, S.A. (2001). The ENT family of eukaryote nucleoside and nucleobase transporters: recent advances in the investigation of structure/function relationships and the identification of novel isoforms. Molecular membrane biology *18*, 53-63.

Ibarra, K.D., and Pfeiffer, J.K. (2009). Reduced ribavirin antiviral efficacy via nucleoside transporter-mediated drug resistance. Journal of virology *83*, 4538-4547.

Jennings, L.L., Hao, C., Cabrita, M.A., Vickers, M.F., Baldwin, S.A., Young, J.D., and Cass, C.E. (2001). Distinct regional distribution of human equilibrative nucleoside transporter proteins 1 and 2 (hENT1 and hENT2) in the central nervous system. Neuropharmacology *40*, 722-731.

Kang, N., Jun, A.H., Bhutia, Y.D., Kannan, N., Unadkat, J.D., and Govindarajan, R. (2010). Human equilibrative nucleoside transporter-3 (hENT3) spectrum disorder mutations impair nucleoside transport, protein localization, and stability. The Journal of biological chemistry *285*, 28343-28352.

Keil, G.J., 2nd, and Delander, G.E. (1995). Time-dependent antinociceptive interactions between opioids and nucleoside transport inhibitors. The Journal of pharmacology and experimental therapeutics *274*, 1387-1392.

Klyuch, B.P., Dale, N., and Wall, M.J. (2012). Deletion of ecto-5'-nucleotidase (CD73) reveals direct action potential-dependent adenosine release. The Journal of neuroscience : the official journal of the Society for Neuroscience *32*, 3842-3847.

Kohler, J.J., and Lewis, W. (2007). A brief overview of mechanisms of mitochondrial toxicity from NRTIs. Environmental and molecular mutagenesis *48*, 166-172.

Kong, W., Engel, K., and Wang, J. (2004). Mammalian nucleoside transporters. Current drug metabolism *5*, 63-84.

Lai, Y., Tse, C.M., and Unadkat, J.D. (2004). Mitochondrial expression of the human equilibrative nucleoside transporter 1 (hENT1) results in enhanced mitochondrial toxicity of antiviral drugs. The Journal of biological chemistry *279*, 4490-4497.

Landolt, H.P. (2008). Sleep homeostasis: a role for adenosine in humans? Biochemical pharmacology *75*, 2070-2079.

Langer, D., Hammer, K., Koszalka, P., Schrader, J., Robson, S., and Zimmermann, H. (2008). Distribution of ectonucleotidases in the rodent brain revisited. Cell and tissue research *334*, 199-217.

Latini, S., and Pedata, F. (2001). Adenosine in the central nervous system: release mechanisms and extracellular concentrations. Journal of neurochemistry *79*, 463-484.

Lefkowitz, R.J. (2004). Historical review: a brief history and personal retrospective of seven-transmembrane receptors. Trends in pharmacological sciences *25*, 413-422.

Li, B., Gu, L., Hertz, L., and Peng, L. (2013). Expression of nucleoside transporter in freshly isolated neurons and astrocytes from mouse brain. Neurochemical research *38*, 2351-2358.

Li, J.Y., Boado, R.J., and Pardridge, W.M. (2001). Cloned blood-brain barrier adenosine transporter is identical to the rat concentrative Na+ nucleoside cotransporter CNT2. Journal of cerebral blood flow and metabolism : official journal of the International Society of Cerebral Blood Flow and Metabolism *21*, 929-936.

Lovatt, D., Xu, Q., Liu, W., Takano, T., Smith, N.A., Schnermann, J., Tieu, K., and Nedergaard, M. (2012). Neuronal adenosine release, and not astrocytic ATP release, mediates feedback inhibition of excitatory activity. Proceedings of the National Academy of Sciences of the United States of America *109*, 6265-6270.

Lu, H., Chen, C., and Klaassen, C. (2004). Tissue distribution of concentrative and equilibrative nucleoside transporters in male and female rats and mice. Drug metabolism and disposition: the biological fate of chemicals *32*, 1455-1461.

Mackey, J.R., Jennings, L.L., Clarke, M.L., Santos, C.L., Dabbagh, L., Vsianska, M., Koski, S.L., Coupland, R.W., Baldwin, S.A., Young, J.D., *et al.* (2002). Immunohistochemical variation of human equilibrative nucleoside transporter 1 protein in primary breast cancers. Clinical cancer research : an official journal of the American Association for Cancer Research *8*, 110-116.

Mani, R.S., Hammond, J.R., Marjan, J.M., Graham, K.A., Young, J.D., Baldwin, S.A., and Cass, C.E. (1998). Demonstration of equilibrative nucleoside transporters (hENT1 and hENT2) in nuclear envelopes of cultured human choriocarcinoma (BeWo) cells by functional reconstitution in proteoliposomes. The Journal of biological chemistry *273*, 30818-30825.

McKenzie, R., Fried, M.W., Sallie, R., Conjeevaram, H., Di Bisceglie, A.M., Park, Y., Savarese, B., Kleiner, D., Tsokos, M., Luciano, C., *et al.* (1995). Hepatic failure and lactic acidosis due to fialuridine (FIAU), an investigational nucleoside analogue for chronic hepatitis B. The New England journal of medicine *333*, 1099-1105.

Molho-Pessach, V., Agha, Z., Aamar, S., Glaser, B., Doviner, V., Hiller, N., Zangen, D.H., Raas-Rothschild, A., Ben-Neriah, Z., Shweiki, S., *et al.* (2008a). The H syndrome: a genodermatosis characterized by indurated, hyperpigmented, and hypertrichotic skin with systemic manifestations. Journal of the American Academy of Dermatology *59*, 79-85.

Molho-Pessach, V., Lerer, I., Abeliovich, D., Agha, Z., Abu Libdeh, A., Broshtilova, V., Elpeleg, O., and Zlotogorski, A. (2008b). The H syndrome is caused by mutations in the nucleoside transporter hENT3. American journal of human genetics *83*, 529-534.

Morgan, N.V., Morris, M.R., Cangul, H., Gleeson, D., Straatman-Iwanowska, A., Davies, N., Keenan, S., Pasha, S., Rahman, F., Gentle, D., *et al.* (2010). Mutations in SLC29A3, encoding an equilibrative nucleoside transporter ENT3, cause a familial histiocytosis syndrome (Faisalabad histiocytosis) and familial Rosai-Dorfman disease. PLoS genetics *6*, e1000833.

Nishio, R., Tsuchiya, H., Yasui, T., Matsuura, S., Kanki, K., Kurimasa, A., Hisatome, I., and Shiota, G. (2011). Disrupted plasma membrane localization of equilibrative nucleoside transporter 2 in the chemoresistance of human pancreatic cells to gemcitabine (dFdCyd). Cancer science *102*, 622-629.

Osato, D.H., Huang, C.C., Kawamoto, M., Johns, S.J., Stryke, D., Wang, J., Ferrin, T.E., Herskowitz, I., and Giacomini, K.M. (2003). Functional characterization in yeast of genetic variants in the human equilibrative nucleoside transporter, ENT1. Pharmacogenetics *13*, 297-301.

Parkinson, F.E., Zhang, Y.W., Shepel, P.N., Greenway, S.C., Peeling, J., and Geiger, J.D. (2000). Effects of nitrobenzylthioinosine on neuronal injury, adenosine levels, and adenosine receptor activity in rat forebrain ischemia. Journal of neurochemistry *75*, 795-802.

Phillis, J.W., O'Regan, M.H., and Walter, G.A. (1989). Effects of two nucleoside transport inhibitors, dipyridamole and soluflazine, on purine release from the rat cerebral cortex. Brain research *481*, 309-316.

Phillis, J.W., and Wu, P.H. (1981). The role of adenosine and its nucleotides in central synaptic transmission. Progress in neurobiology *16*, 187-239.

Picano, E., and Abbracchio, M.P. (2000). Adenosine, the imperfect endogenous anti-ischemic cardio-neuroprotector. Brain research bulletin *52*, 75-82.

Post, C. (1984). Antinociceptive effects in mice after intrathecal injection of 5'-N-ethylcarboxamide adenosine. Neuroscience letters *51*, 325-330.

Priya, T.P., Philip, N., Molho-Pessach, V., Busa, T., Dalal, A., and Zlotogorski, A. (2010). H syndrome: novel and recurrent mutations in SLC29A3. The British journal of dermatology *162*, 1132-1134.

Reyes, G., Naydenova, Z., Abdulla, P., Chalsev, M., Villani, A., Rose, J.B., Chaudary, N., DeSouza, L., Siu, K.W., and Coe, I.R. (2010). Characterization of mammalian equilibrative nucleoside transporters (ENTs) by mass spectrometry. Protein expression and purification *73*, 1-9.

Safran, N., Shneyvays, V., Balas, N., Jacobson, K.A., Nawrath, H., and Shainberg, A. (2001). Cardioprotective effects of adenosine A1 and A3 receptor activation during hypoxia in isolated rat cardiac myocytes. Molecular and cellular biochemistry *217*, 143-152.

Sebastiao, A.M., and Ribeiro, J.A. (2000). Fine-tuning neuromodulation by adenosine. Trends in pharmacological sciences *21*, 341-346.

Song, D., Xu, J., Bai, Q., Cai, L., Hertz, L., and Peng, L. (2014). Role of the Intracellular Nucleoside Transporter ENT3 in Transmitter and High K(+) Stimulation of Astrocytic ATP Release Investigated Using siRNA Against ENT3. ASN neuro *6*, 1759091414543439.

Spiegel, R., Cliffe, S.T., Buckley, M.F., Crow, Y.J., Urquhart, J., Horovitz, Y., Tenenbaum-Rakover, Y., Newman, W.G., Donnai, D., and Shalev, S.A. (2010). Expanding the clinical spectrum of SLC29A3 gene defects. European journal of medical genetics *53*, 309-313.

Stone, T.W., Forrest, C.M., Mackay, G.M., Stoy, N., and Darlington, L.G. (2007). Tryptophan, adenosine, neurodegeneration and neuroprotection. Metabolic brain disease *22*, 337-352.

Sundaram, M., Yao, S.Y., Ingram, J.C., Berry, Z.A., Abidi, F., Cass, C.E., Baldwin, S.A., and Young, J.D. (2001). Topology of a human equilibrative, nitrobenzylthioinosine (NBMPR)-sensitive nucleoside transporter (hENT1) implicated in the cellular uptake of adenosine and anti-cancer drugs. The Journal of biological chemistry *276*, 45270-45275.

Svenningsson, P., Le Moine, C., Fisone, G., and Fredholm, B.B. (1999). Distribution, biochemistry and function of striatal adenosine A2A receptors. Progress in neurobiology *59*, 355-396.

Valdes, R., Casado, F.J., and Pastor-Anglada, M. (2002). Cell-cycle-dependent regulation of CNT1, a concentrative nucleoside transporter involved in the uptake of cell-cycle-dependent nucleoside-derived anticancer drugs. Biochemical and biophysical research communications *296*, 575-579.

Volonte, C., and D'Ambrosi, N. (2009). Membrane compartments and purinergic signalling: the purinome, a complex interplay among ligands, degrading enzymes, receptors and transporters. The FEBS journal *276*, 318-329.

Wall, M., and Dale, N. (2008). Activity-dependent release of adenosine: a critical re-evaluation of mechanism. Current neuropharmacology *6*, 329-337.

Wall, M.J., Atterbury, A., and Dale, N. (2007). Control of basal extracellular adenosine concentration in rat cerebellum. The Journal of physiology *582*, 137-151.

Wall, M.J., and Dale, N. (2007). Auto-inhibition of rat parallel fibre-Purkinje cell synapses by activity-dependent adenosine release. The Journal of physiology *581*, 553-565.

Wall, M.J., and Dale, N. (2013). Neuronal transporter and astrocytic ATP exocytosis underlie activity-dependent adenosine release in the hippocampus. The Journal of physiology *591*, 3853-3871.

Ward, J.L., Sherali, A., Mo, Z.P., and Tse, C.M. (2000). Kinetic and pharmacological properties of cloned human equilibrative nucleoside transporters, ENT1 and ENT2, stably expressed in nucleoside transporter-deficient PK15 cells. Ent2 exhibits a low affinity for guanosine and cytidine but a high affinity for inosine. The Journal of biological chemistry *275*, 8375-8381.

Wong, A.Y., Billups, B., Johnston, J., Evans, R.J., and Forsythe, I.D. (2006). Endogenous activation of adenosine A1 receptors, but not P2X receptors, during high-frequency synaptic transmission at the calyx of Held. Journal of neurophysiology *95*, 3336-3342.

Young, J.D., Yao, S.Y., Baldwin, J.M., Cass, C.E., and Baldwin, S.A. (2013). The human concentrative and equilibrative nucleoside transporter families, SLC28 and SLC29. Molecular aspects of medicine *34*, 529-547.

Zhang, J., Visser, F., King, K.M., Baldwin, S.A., Young, J.D., and Cass, C.E. (2007). The role of nucleoside transporters in cancer chemotherapy with nucleoside drugs. Cancer metastasis reviews *26*, 85-110.

Zhou, M., Duan, H., Engel, K., Xia, L., and Wang, J. (2010). Adenosine transport by plasma membrane monoamine transporter: reinvestigation and comparison with organic cations. Drug metabolism and disposition: the biological fate of chemicals *38*, 1798-1805.

Zimmermann, H. (1996). Biochemistry, localization and functional roles of ecto-nucleotidases in the nervous system. Progress in neurobiology *49*, 589-618.